Crosslinked Extracellular Matrix Stiffens Human Trabecular Meshwork Cells Via Dysregulating β-catenin and YAP/TAZ Signaling Pathways

Felix Yemanyi,[1] Janice Vranka,[2] and Vijay Krishna Raghunathan[1,3]

[1]Department of Basic Sciences, College of Optometry, University of Houston, Houston, TX, United States
[2]Casey Eye Institute, Oregon Health and Science University, Portland, OR, United States
[3]Department of Biomedical Engineering, Cullen College of Engineering, University of Houston, Houston, TX, United States

Correspondence: Vijay Krishna Raghunathan, Department of Basic Sciences, College of Optometry, University of Houston, 4901 Calhoun Road, Houston, TX 77204, USA; vraghunathan@uh.edu.

Received: May 6, 2020
Accepted: August 5, 2020
Published: August 24, 2020

Citation: Yemanyi F, Vranka J, Raghunathan VK. Crosslinked extracellular matrix stiffens human trabecular meshwork cells via dysregulating β-catenin and YAP/TAZ signaling pathways. *Invest Ophthalmol Vis Sci.* 2020;61(10):41. https://doi.org/10.1167/iovs.61.10.41

Purpose. The purpose of this study was to determine whether genipin-induced crosslinked cell-derived matrix (XCDM) precipitates fibrotic phenotypes in human trabecular meshwork (hTM) cells by dysregulating β-catenin and Yes-associated protein (YAP)/transcriptional coactivator with PDZ-binding motif (TAZ) signaling pathways.

Methods. Cell-derived matrices were treated with control or genipin for 5 hours to obtain respective uncrosslinked (CDM) and XCDMs and characterized. hTM cells were seeded on these matrices with/without Wnt pathway modulators in serum-free media for 24 hours. Elastic modulus, gene, and protein (whole cell and subcellular fractions) expressions of signaling mediators and targets of Wnt/β-catenin and YAP/TAZ pathways were determined.

Results. At the highest genipin concentration (10% XCDM), XCDM had increased immunostaining of N-ε(γ-glutamyl)-lysine crosslinks, appeared morphologically fused, and was stiffer (5.3-fold, $P < 0.001$). On 10% XCDM, hTM cells were 7.8-fold ($P < 0.001$) stiffer, total β-catenin was unchanged, pβ-catenin was elevated, and pGSK3β was suppressed. Although 10% XCDM had no effect on cytoplasmic β-catenin levels, it reduced nuclear β-catenin, cadherin 11, and key Wnt target genes/proteins. The 10% XCDM increased total TAZ, decreased pTAZ, and increased cytoplasmic TAZ levels in hTM cells. The 10% XCDM increased total YAP, reduced nuclear YAP levels, and critical YAP/TAZ target genes/proteins. Wnt activation rescued hTM cells from 10% XCDM-induced stiffening associated with increased nuclear β-catenin.

Conclusions. Increased cytoplasmic TAZ may inhibit β-catenin from its nuclear shuttling or regulating cadherin 11 important for aqueous homeostasis. Elevated cytoplasmic TAZ may inhibit YAP's probable homeostatic function in the nucleus. Together, TAZ's cytoplasmic localization may be an important downstream event of how increased TM extracellular matrix (ECM) crosslinking may cause increased stiffness and ocular hypertension in vivo. However, Wnt pathway activation may ameliorate ocular hypertensive phenotypes induced by crosslinked ECM.

Keywords: extracellular matrix, trabecular meshwork, crosslinking, Wnt, β-catenin, YAP/TAZ, Mechanotransduction

Primary open angle glaucoma (POAG), an optic neuropathy, is a leading cause of global irreversible vision loss,[1–3] and ocular hypertension is its only modifiable predominant risk factor.[4] Ocular hypertension arises from increased resistance to aqueous outflow at the trabecular meshwork (TM),[5–8] which is its primary egress, in the anterior chamber of the eye. Although TM changes implicated in ocular hypertension are multifactorial,[9–12] aberrant TM extracellular matrix (ECM) remodeling is considered a primary contributory factor.[8,13–20] One major component of TM ECM changes implicated in ocular hypertension and glaucoma is the increased expression and activity of ECM crosslinking enzymes like lysyl oxidase (LOX), LOX-like 1 to 4, and tissue transglutaminase 2 (TGM2).[21–26] For example, Raychaudhuri and colleagues[23] showed overexpression of TGM2, to induce crosslinks in the TM ECM, caused ocular hypertension in mice; conversely, TGM2-knockout mice had markedly reduced ocular hypertension.[24] Yang and colleagues[25] also reported LOX-dependent induction or inhibition of TM ECM crosslinking reduced or increased outflow facility, respectively, in perfused human and porcine anterior segment organ cultures. These enzymes enhance irreversible covalent crosslinking of major ECM structural proteins, like fibronectin, collagen, and elastin[27–29]; thereby making the latter resistant to proteolytic degradation by

matrix metalloproteinases (MMPs) as part of a homeostatic response. This may subsequently lead to decreased ECM turnover and ECM accumulation, increased ECM stiffness, elevated aqueous outflow resistance, and ocular hypertension.[15,19,30] However, the underlying downstream mechanism(s) by which a crosslinked TM ECM induces ocular hypertensive phenotypes in cells requires further studies.

A crosslinked TM ECM may hinder outflow facility via its deleterious interaction with resident human TM (hTM) cells; wherein the latter is driven toward a pathological state, losing their homeostatic function in draining aqueous humor. Increased ECM crosslinking confers stability and increased stiffness to several non-ocular tissues/scaffolds.[31–33] Thus, via mechanotransduction, hTM cells may translate biophysical stimuli like altered topography and increased stiffness from a crosslinked ECM into biochemical signals to instruct changes in behavior/function. Two well-established mechanotransduction pathways that could serve as critical regulatory nodes in hTM cells in the event of increased ECM crosslinking are Wnt/β-catenin and Yes-associated protein (YAP)/transcriptional coactivator with PDZ-binding motif (TAZ). These mechanotransducers have been implicated in development, tissue homeostasis, tissue repair/regeneration, and disease.[34–37] Further, largely in response to chemical ligands, synergistic/inhibitory bidirectional interactions between β-catenin and YAP/TAZ signaling pathways have been documented in different cells and tissues.[38–44] Because the functions of these signaling pathways are ligand- and biological context-dependent,[35,39,41,45,46] it is imperative to document their probable relative modulation in hTM cells in response to relevant biophysical stimuli. However, previous studies implicating β-catenin and YAP/TAZ signaling pathways in aqueous homeostasis and/or ocular hypertensive phenotypes (i) focused on an individual signaling pathway,[47–50] (ii) activated/inhibited either the Wnt/β-catenin or the YAP/TAZ pathways solely with chemical ligands,[50–52] (iii) did not quantify subcellular localization of signaling molecules,[47,51,52] and/or (iv) seeded cells on plastic and/or polymeric substrates that are limited in their recapitulation of in vivo ECM.[47,51,52]

In view of the above, we hypothesized that increased TM ECM crosslinking precipitates ocular hypertensive phenotypes (for instance, increased cell/tissue stiffness) in hTM cells by dysregulating two key mechanotransduction pathways implicated in ocular hypertension and glaucoma: β-catenin and/or YAP/TAZ signaling pathways. To test this hypothesis, first, we characterized and validated genipin-induced crosslinking of TM cell-derived matrices (XCDMs) biochemically, morphologically, and biomechanically. We used genipin (a natural collagen crosslinker) in our studies because it mimics LOX in its crosslinking mechanism[27,53,54] and it is 10,000 times less cytotoxic than glutaraldehyde, another potent crosslinker.[53,55] Next, we documented the effect XCDMs have on hTM cell biomechanics associated with changes in β-catenin and YAP/TAZ signaling pathways using RNA, whole cell lysates, and nuclear/cytoplasmic fractions. Finally, because Wnt/β-catenin pathway antagonism is implicated in cell stiffening,[50] we determined the effect of activating this pathway on the stiffness of hTM cells seeded on XCDMs. A portion of the experimental outcomes of this study has been reported as an abstract elsewhere.[56]

Materials and Methods

Isolation of Human Trabecular Meshwork and Subsequent Cell Culture

Primary hTM cells were carefully dissected from donor corneoscleral rims unsuitable for transplant (SavingSight Eye Bank, St. Louis, MO, USA), as described previously.[57] TM rings cut into pieces were placed with 0.2% (w/v) collagen coated cytodex beads in complete growth medium (Dulbecco's modified Eagle medium/Nutrient Mixture F-12 [50:50; DMEM/F-12] with 2.5 mM L-glutamine supplemented with 10% fetal bovine serum [FBS], and 1% penicillin/amphotericin [Life Technologies, Carlsbad, CA, USA]). Subsequently, cells that moved out of the TM were cultured in complete growth media and used between passages two (2) and six (6). For characterization of primary hTM cells, all cell strains were probed for dexamethasone (DEX)-induced expression of myocilin as recommended (Supplementary Figure S1).[58] This study is not deemed a human subject research because cells were acquired post-mortem from de-identified donor tissues and is thus University of Houston Institutional Review Board (IRB) exempt. However, all experiments were conducted in accordance with the tenets of the Declaration of Helsinki. Donor demographics are as follows: 57F, female, age 57 years; 73M, male, age 73 years; 74M, male, 74 years; and 75F, female, age 75 years.

Generation of Vehicle Control and Genipin-Induced Crosslinked TM CDMs from Cultured hTM Cells

As previously described,[59] primary hTM cells were cultured in sterile pretreated 60 mm dishes (5,000–10,000 cells per cm^2) and amino-silane modified 12 mm glass coverslips in a 24-well culture plate (5,000–10,000 cells per cm^2) in complete growth media for 4 weeks, changing growth media on every other day. Subsequently, a decellularization buffer consisting of 20 mM ammonium hydroxide, 0.05% Triton X-100 and deionized water[60] was used to remove resident cells from their deposited ECMs to obtain pristine TM cell-derived matrices (CDMs). These CDMs were incubated with 50 U/mL DNase I and RNase A for 2 hours and washed thoroughly in Hank's balanced salt solution (HBSS). Simultaneously, a stock solution of 5% (w/v) genipin (catalog number: 078-03021; FUJIFILM Wako Chemicals, Richmond, VA, USA) was prepared by dissolution in dimethyl sulfoxide (DMSO). Working solutions of genipin was prepared by dilution of the 5% (w/v) stock solution in phosphate buffered saline (PBS) by 100-, 50- or 10-fold to obtain 1% (v/v), 2% (v/v), and 10% (v/v) solutions. Matrices were incubated in PBS alone, or 1% (v/v), 2% (v/v), and 10% (v/v) genipin solutions for 5 hours to generate uncrosslinked vehicle control (CDM) and 1% (1% XCDM), 2% (2% XCDM), and 10% (10% XCDM) genipin-induced crosslinked TM CDMs, respectively. Uncrosslinked CDMs and XCDMs were characterized via immunocytochemistry, scanning electron microscopy, and atomic force microscopy prior to subsequent cell culture.

Biochemical Characterization of CDM and XCDMs by Immunocytochemistry

After thorough PBS washes, appropriate decellularized vehicle control CDM, 1%, 2%, and 10% XCDMs on glass coverslips were fixed with 4% paraformaldehyde in PBS at 4°C for

Investigative Ophthalmology & Visual Science

30 minutes. Then, samples were washed three times, 5 minutes each with PBS and with 0.25% Triton X-100 in PBS (pH 7.4) for 10 minutes. Following three washes, each lasting for 5 minutes, samples were blocked in 5% bovine serum albumin (BSA) in PBS for 30 minutes. Subsequently, samples were incubated overnight at 4°C with primary antibodies; anti-N epsilon gamma glutamyl Lysine (GGEL; catalog number: ab424; Abcam, Cambridge, MA, USA), and/or anti-Laminin (catalog number, ab11575; Abcam), anti-Fibronectin (catalog number: ab2413; Abcam) or anti-Collagen IV (catalog number: ab6311; Abcam), respectively, at 1/250 dilution in 5% BSA/PBS (primary antibodies were omitted as negative controls; data not shown). After three 5-minute washes in PBS the following day, samples were incubated with species-appropriate fluorophore-tagged secondary antibodies (Alexa Fluor 488 and 594, Anti-Rabbit and Anti-Mouse; Thermo Fisher Scientific) at respective 1/500 dilution at room temperature for 1 hour. Following three 5-minute washes, samples were counterstained with 4'6-diamidino-2-phenylindole (DAPI; catalog number: D1306; Fisher Scientific, Pleasanton, CA, USA) at 1/10,000 dilution for 5 minutes. After a single 5-minute wash, glass coverslips were mounted with Fluoromount-G Mounting Medium (catalog number: 0100-01; Southern Biotech, Birmingham, AL, USA) onto slides. Immunofluorescent images were then captured with Zeiss LSM 800 laser scanning confocal microscope (Carl Zeiss, Jena, Germany) or Leica DMi8 inverted fluorescent microscope (Leica Microsystems AG, Germany) with a 20 x objective. For each immunolabeled sample, 5 to 10 random locations were imaged. At least two to three samples were used for each immunolabeling condition for each cell strain with the same imaging settings for cohorts.

Morphological Characterization of CDM and XCDMs by Scanning Electron Microscopy

Decellularized uncrosslinked CDM, 1%, 2%, and 10% XCDMs on glass coverslips were washed thoroughly with distilled water. Samples were then serially dehydrated in ethanol and hexamethyldisilazane (HMDS; catalog number: 440191; Sigma Aldrich, St. Louis, MO, USA). Specifically, this involved samples' sequential incubation in 30%, 50%, and 70% ethanol for 5 minutes each at room temperature. Then, further dehydration was done in 90% ethanol twice, each for 5 minutes; followed by samples' incubation in 100% ethanol three times, each for 5 minutes. Then, decellularized samples were further dehydrated in a 1:1 mixture of 100% ethanol and HMDS for 10 minutes. Afterward, they were incubated in HMDS two times, for 10 minutes each. Samples were subsequently incubated in HMDS overnight under a laminar flow hood to dry. They were then sputter coated with gold to enhance conductivity, reduce sample charging, and increase resolution during imaging. Surface topography of CDM, 1%, 2%, and 10% XCDMs were then imaged using a MIRA3 field emission scanning electron microscope (SEM; TESCAN, Pittsburgh, PA, USA). The same imaging criteria involving a sample area of 10 x 10 µm, voltage of 12 kV, and a magnification of 55,300 x were used for all samples. For each experimental sample, at least five random areas were captured. At least two to three samples were used for each experimental condition for each cell strain. Representative electron micrograph is shown for each condition.

Biomechanical Characterization of CDM and XCDMs by Atomic Force Microscopy

Stiffness of vehicle control CDM, 1%, 2%, and 10% XCDMs on glass coverslips was determined by atomic force microscopy (AFM) after equilibrating all samples in HBSS for 30 minutes and cantilever calibration via thermal tuning as described previously.[14,61] Briefly, force-indentation curves were obtained in contact mode using a silicon nitride PNP-TR cantilever (nominal spring constant 0.32 N/m; NanoAndMore, Lady's Island, SC, USA) modified with 10 µm diameter borosilicate bead (Thermo Fisher Scientific). For all samples, force-indentation curves were obtained with this colloidal probe from at least 10 random locations; with at least 5 force-indentation curves obtained per location. Elastic modulus of each sample was subsequently determined by fitting the respective generated force-indentation curves with Hertz model for spherical indenter within a linearly elastic region of the sample. Given their high-water content, all biologic samples were assumed as incompressible materials with an assumed Poisson's ratio of 0.5. Finally, all the individual elastic modulus obtained were averaged for each sample ($n = 4$ biological replicates).

Cell Culture on CDM and XCDMs

Vehicle control CDM and XCDMs (on glass coverslips or dishes) obtained were primed with serum-free media at room temperature for approximately 4 hours. After removing the media, low passage hTM cells from the same donor used to derive ECMs were seeded (5,000–10,000 per cm^2) on CDM or 1%, 2%, and/or 10% XCDMs in serum-free media for 24 hours. In other parallel experiments, hTM cells were cultured on CDM or 10% XCDM in serum-free media for 24 hours, with or without 250 nM Wnt signaling activator, LY2090314 (Selleckchem, Houston, TX, USA) or 10 µM Wnt signaling inhibitor, LGK974 (Selleckchem, Houston, TX, USA). Subsequently, in subsets of these experiments, cell mechanics was determined via AFM, RNA was extracted for reverse transcriptase-quantitative polymerase chain reaction (RT-qPCR), and protein was extracted from whole cell lysates/subcellular fractions for Western blotting.

Measurement of Cell Stiffness by Atomic Force Microscopy

Mechanics of hTM cells seeded on CDM or 1%, 2%, and 10% XCDMs for 24 hours was determined via AFM, as described previously.[14,20,61,62] The same was done for another experiment in which hTM cells were cultured on CDM or 10% XCDM for 24 hours in the presence or absence of 250 nM Wnt pathway activator. Briefly, PNP-TR cantilever with a pyramidal tip (nominal spring constant 0.32 N/m; Nano and More) was used without any modification to its tip geometry. The deflection sensitivity and spring' constant of the cantilever were calibrated via instrument software before obtaining measurements. Further, samples were also calibrated and equilibrated in HBSS for 30 minutes, before taking at least 5 force-indentation curves for any random cell in contact mode. This was repeated for at least nine other random cells per experimental sample. Data were subsequently analyzed using a custom semi-automated Matlab program adapting analytical principles previously described.[63] For instance, automated restriction of cantilever's indentation to the linear elastic region of the

Investigative Ophthalmology & Visual Science

biologic sample, using a Poisson ratio of 0.5 for incompressible biologic samples, and fitting the curve with a Sneddon model.

RNA Extraction and Quantitative Real-Time PCR

Total RNA was isolated from hTM cells that had been cultured on CDM or 1%, 2%, and 10% XCDMs in 60 mm dishes for 24 hours using an RNA purification kit (catalog number: 12183025; PureLink RNA Mini kit, Invitrogen, Carlsbad, CA). Using the High-Capacity cDNA Reverse Transcription Kit (catalog number: 4368813; Applied Biosystems, Foster City, CA), 1 µg of total RNA was used to synthesize cDNA following the manufacturer's instructions. Quantitative real-time polymerase chain reaction (qPCR) was performed on 20 ng of the cDNA with specific primers (Supplementary Table S1) with PowerUp SYBR Green Master Mix kit (catalog number: A25918; Applied Biosystems, Foster City, CA) in total volumes of 10 µL per reaction using a CFX Connect Real-time System from Bio-Rad Laboratories (Bio-Rad, Hercules, CA, USA). The cycle threshold (Ct) values were obtained from the qPCR equipment and exported into Microsoft Excel for subsequent analysis using the $2^{-\Delta\Delta Ct}$ method, with glyceraldehyde 3-phosphate dehydrogenase (GAPDH) as the internal control gene.

Protein Extraction and Subsequent Western Blotting

Primary hTM cells were seeded on CDM or 1%, 2%, and/or 10% XCDMs in 60 mm dishes for 24 hours. In another experiment, cells were seeded on CDM or 10% XCDM for 24 hours in the presence or absence of 250 nM Wnt pathway activator or 10 µM Wnt pathway inhibitor. Whole cells were lysed and scraped into radioimmunoprecipitation assay (RIPA) buffer (ThermoScientific, Waltham, MA, USA) supplemented with protease and phosphatase inhibitors (Fisher Scientific, Hampton, NH, USA) on ice, and then subsequently centrifuged at 12,000 g for 15 minutes at 4°C to pellet and exclude cellular debris. In parallel, NE-PER nuclear and cytoplasmic reagent kit (catalog number: 78835; Thermo Fisher Scientific) was used to separate a subset of whole cells into their nuclear and cytoplasmic fractions following the manufacturer's instructions. Subsequently, supernatants from whole cell lysates and cell nuclear/cytoplasmic fractions were transferred into fresh clean tubes and quantified via a modified Lowry assay (DC assay; Biorad, Hercules, CA, USA) with BSA as the standard. Protein lysates were subsequently denatured in a 1:10 mixture of 2-mercaptoethanol and 4 x Laemmli buffer by boiling at 100°C for 5 minutes. After quickly centrifuging proteins at 15,000 g for 30 seconds, equal amounts of protein were loaded per well (20 µg) for each sample and ran on denaturing 4 to 15% gradient polyacrylamide ready-made gels (Biorad); then transferred onto polyvinylidene difluoride (PVDF) membranes by electrophoresis. Membrane blots were blocked in 5% BSA in 1 x tris buffered saline/tween-20 (TBST) for 1 hour. Immunoblots were incubated overnight at 4°C with specific primary antibodies (Supplementary Table S2) on a rotating shaker. The membrane blot was washed three times with TBST; each wash lasting for approximately 10 minutes. Subsequent incubation with corresponding HRP-conjugated species-specific secondary antibodies (Supplementary Table S2) for 45 minutes was done, followed by three 10-minute washes with TBST. The protein bands were then visualized using ECL detection reagents (SuperSignal West Femto Maximum Sensitivity Substrate; Life Technologies, Grand Island, NY, USA) and imaged with a Bio-Rad ChemiDoc MP imaging system. Respective membrane blots were stripped and probed with GAPDH and/or Lamin A/C as housekeeping proteins. Data were exported into ImageJ software for densitometric analysis.

Statistics

For cell mechanics data, gene and protein expression data, 1-way ANOVA followed by Tukey multiple comparisons post hoc test was used for analysis, with P values less than 0.05 considered to be statistically significant. All data are presented as mean ± standard error of the mean (SEM) in bar graphs, representative confocal/scanning electron micrographs and blots where applicable.

Results

Ten Percent XCDM Showed Most Increased Immunostaining/Colocalization for a Crosslinking Marker and Major ECM Structural Proteins

Prior to investigating alterations in mechanotransduction pathways that could be perturbed in hTM cells cultured on XCDMs, we validated genipin's potency to crosslink TM CDMs via immunocytochemistry. Compared with uncrosslinked control CDMs, we observed that 10% genipin-induced XCDM (10% XCDM) had a profound increase in immunostaining of N-ε(γ-glutamyl) lysine (GGEL) crosslinks (Fig. 1A), that co-localized with the basement membrane protein, laminin (Fig. 1B). In addition, overlap in signal intensity for major ECM structural proteins, fibronectin, and collagen IV, increased with genipin-induced crosslinking of CDMs. Specifically, 10% XCDM had more intensity overlap for these ECM proteins compared with 2% XCDM, 1% XCDM, or uncrosslinked control CDM (Fig. 1C).

Ten Percent XCDM Appeared to be "Fused" Morphologically and Emerged as the Stiffest

Given genipin's role in altering different tissues morphologically and/or biomechanically,[33,64,65] we next characterized the morphology and stiffness of genipin-induced XCDMs by scanning electron microscopy and atomic force microscopy (using a colloidal probe) respectively. Compared with CDM, 1% XCDM, or 2% XCDM, 10% XCDM appeared to be thicker and more "fused" morphologically (Fig. 2A). Further, significant stiffening of matrices was observed after genipin treatment in a concentration-dependent manner. Specifically, compared with CDM, whereas 1% XCDM was not any different, 2% and 10% XCDMs were 2.4- and 5.3-fold stiffer ($P < 0.001$), respectively (Fig. 2B).

Ten Percent XCDM Profoundly Stiffened Seeded hTM Cells

Considering the relationship between tissue biomechanics and aqueous outflow[19] together with the wealth of evidence on the effect of substratum properties on compliance/function of resident cells,[34,35,47,61,66–68] we next determined the elastic moduli of hTM cells cultured on CDM and

Investigative Ophthalmology & Visual Science

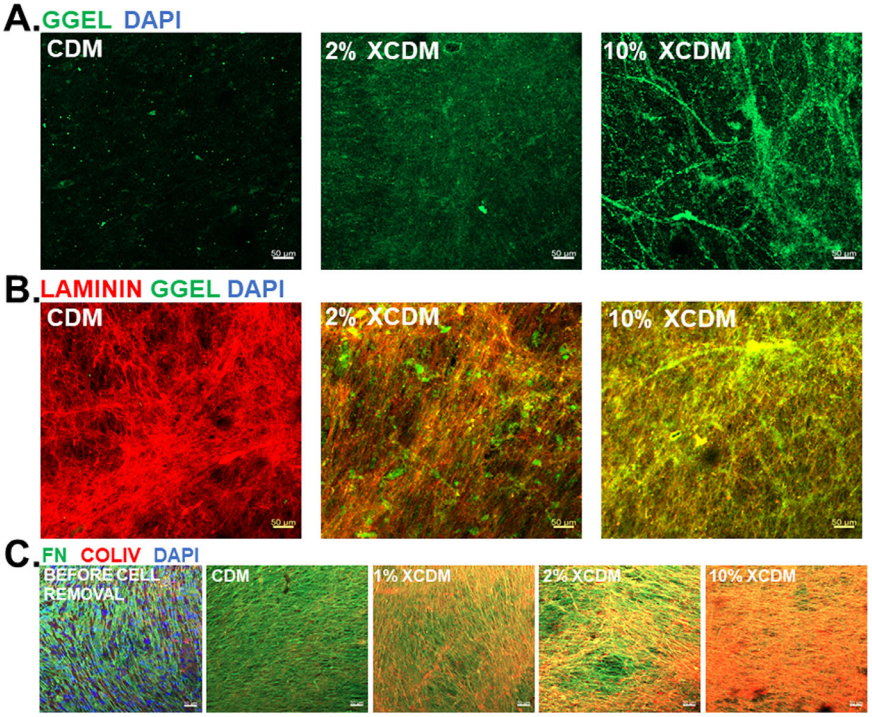

Figure 1. Ten percent (10%) XCDM had the most increased immunostaining/immunolocalization of GGEL crosslinks and major ECM proteins. Ammonium hydroxide (20 mM) decellularization buffer was used to generate cell-derived matrices (CDMs) from primary hTM cells cultured for 4 weeks in complete growth media. After using enzymes to subsequently remove any remaining DNA/RNA, CDMs were treated with vehicle control, 2% or 10% genipin/PBS for 5 hours to obtain vehicle control (CDM), 2% and 10% genipin-induced crosslinked CDMs (2% and 10% XCDMs), respectively, before performing immunocytochemistry. Representative images showing (**A**) CDM, 2%, and 10% XCDMs immunolabeled for N-ε(γ-glutamyl) lysine (GGEL) crosslinks and DAPI (**B**) CDM, 2% and 10% XCDMs immunolabeled for laminin, GGEL, and DAPI. (**C**) Before removal of cells from deposited ECMs after 4 weeks of culture together with decellularized CDM, 1%, 2%, and 10% XCDMs immunolabeled for fibronectin (FN), collagen IV (COLIV), and DAPI ($n = 4$ biological replicates). hTM, human trabecular meshwork; PBS, phosphate buffered saline; DAPI, 4′,6-diamidino-2-phenylindole. Scale bar; 50 µm.

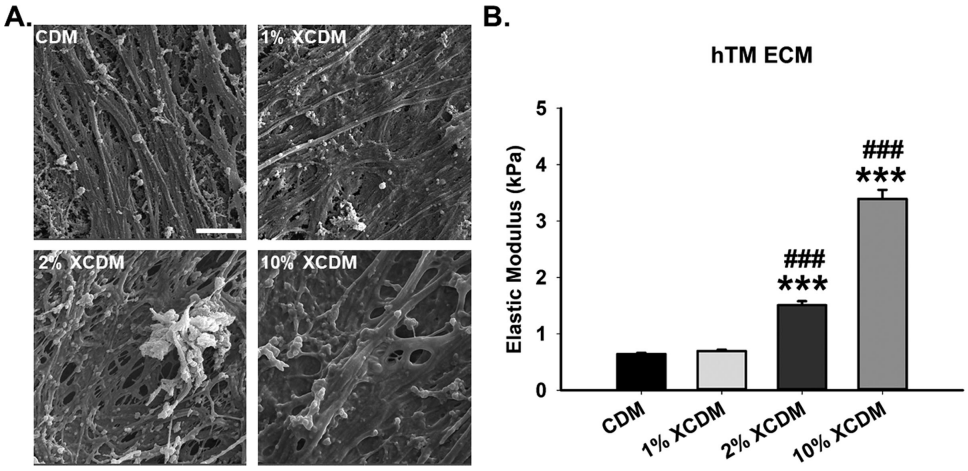

Figure 2. Ten percent (10%) XCDM was most fused morphologically and the stiffest. Cell-derived matrices (CDMs) were generated from hTM cells cultured for 4 weeks in complete growth media using 20 mM ammonium hydroxide decellularization buffer. Subsequently, CDMs were crosslinked with vehicle control, 1%, 2%, and 10% genipin/PBS for 5 hours to obtain vehicle control (CDM), 1%, 2%, and 10% genipin-induced crosslinked CDMs (1%, 2%, and 10% XCDMs, respectively). Before performing scanning electron microscopy, respective samples were dehydrated, and sputter coated. Representative scanning electron micrographs of (**A**) CDM, 1%, 2%, and 10% XCDMs ($n =$ 3 biological replicates). Scale bar; 2 µm. For atomic force microscopy-derived elastic moduli of CDM, 1%, 2%, and 10% XCDMs, a modified PNP-TR cantilever with a 10 µm bead attached to its usual conical tip, was used. At least 5 measurements were taken at any random CDM position; with a total of 10 CDM positions probed for each experimental sample. Bar graph shows elastic moduli of (**B**) CDM, 1%, 2%, and 10% XCDMs. *Columns and error bars*; means and standard error of mean (SEM). One-way ANOVA with the Tukey pairwise comparisons post hoc test was used for statistical analysis ($n =$4 biological replicates. $^{***}P < 0.001$ for the group of interest versus vehicle control, CDM. $^{###}P < 0.001$ for the group of interest versus 1% XCDM). hTM, human trabecular meshwork; PBS, phosphate buffered saline.

Investigative Ophthalmology & Visual Science

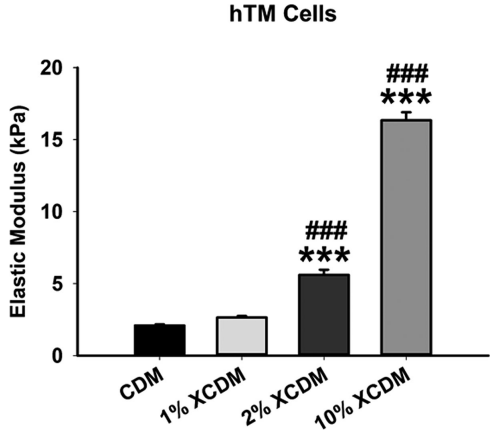

Figure 3. Ten percent (10%) XCDM profoundly stiffened hTM cells. The 20 mM ammonium hydroxide decellularization buffer was used to generate cell-derived matrices (CDMs) from primary hTM cells cultured for 4 weeks in complete growth media. Enzymatic treatment was used to remove any remaining DNA/RNA. Then, CDMs were treated with vehicle control, 1%, 2%, or 10% genipin/PBS for 5 hours to obtain vehicle control (CDM), 1%, 2%, and 10% genipin-induced crosslinked CDMs (1%, 2%, and 10% XCDMs), respectively. New, low passage, hTM cells from the same donor used to obtain CDMs were cultured on uncrosslinked control CDM and XCDMs in serum-free media for 24 hours. Subsequently, cell mechanics was performed via atomic force microscopy using normal PNP-TR cantilevers with conical tips. At least 5 measurements were taken for any random cell; with a total of 10 cells probed for each experimental sample. Bar graph shows elastic moduli of hTM cells seeded on CDM, 1% XCDM, 2% XCDM, and 10% XCDM. *Columns and error bars*; means and standard error of mean (SEM). One-way ANOVA with the Tukey pairwise comparisons post hoc test was used for statistical analysis (n =4 biological replicates). $^{***}P < 0.001$ for the group of interest versus vehicle control, CDM. $^{\#\#\#}P < 0.001$ for the group of interest versus 1% XCDM). hTM, human trabecular meshwork; PBS, phosphate buffered saline.

XCDMs in serum-free media for 24 hours via AFM (using a conical probe). Again, mirroring stiffness of XCDMs, change in cell stiffness was a function of CDM or XCDM stiffness. Compared with hTM cells on control CDM, cells on 2% XCDM were 2.7-fold ($P < 0.001$), whereas cells on 10% XCDM were 7.8-fold ($P < 0.001$) stiffer. No differences in cell stiffness was observed comparing CDM and 1% XCDM (Fig. 3).

Ten Percent XCDM Dysregulated Nucleocytoplasmic Shuttling of β-Catenin in hTM Cells

Since substratum-mediated cell stiffening was observed, we hypothesized that key mechanotransduction pathways could be altered. Consequently, we focused on Wnt/β-catenin signaling pathway owing to its demonstrated roles in mechanotransduction and aqueous homeostasis in previous studies.[35,37,49–51,69,70] Because the function of β-catenin is partly dependent on its relative subcellular localization,[71] we performed Western blotting to quantify protein levels of crucial Wnt/β-catenin pathway mediators using both whole cell lysates and nuclear/cytoplasmic fraction derived from hTM cells cultured on CDM or 1%, 2%, and 10% XCDMs for 24 hours. For whole cell lysates, whereas there were no differences in β-catenin levels among experimental groups (Fig. 4A), phosphorylated β-catenin (pβ-catenin) was significantly overexpressed (2.1-fold, $P < 0.001$) in hTM cells only on 10% XCDM (Fig. 4B) compared with cells on control CDM. In addition, compared with CDM, 2% and 10% XCDMs markedly decreased phosphorylated glycogen synthase kinase-3 beta levels (pGSK3β; -2.0-fold, $P < 0.01$; and -2.5-fold, $P < 0.001$, respectively) in hTM cells (Fig. 4C). Further, whereas subcellular fractionation revealed no significant differences in β-catenin levels in the cytoplasm of hTM cells among groups, only 10% XCDM significantly reduced nuclear β-catenin (-2.5-fold, $P < 0.05$) in hTM cells compared with vehicle CDM (Fig. 4D).

Ten Percent XCDM Downregulated OB-Cadherin Protein in hTM Cells

Because the role of Wnt/β-catenin signaling in maintaining aqueous homeostasis is due in part to its regulation of cell-cell adhesion via mechanosensitive cadherins,[51] we next determined the effect of XCDMs on the gene and protein expression of key cadherins in hTM cells. Compared with uncrosslinked CDM, the gene expression of K-cadherin (cadherin 6) was significantly overexpressed (1.36-fold, 1.43-fold, and 1.36-fold, $P < 0.001$, respectively) in hTM cells cultured on 1%, 2%, and 10% XCDMs (Fig. 5A). Similarly, the gene expression of OB-cadherin (cadherin 11) was markedly increased (2.6-fold, $P < 0.05$; and 3.7-fold, $P < 0.001$, respectively) in hTM cells on 1% and 2% XCDMs, but unchanged on 10% XCDM, compared with control CDM (Fig. 5B). Further, no marked differences in N-cadherin gene levels (cadherin 2) among groups were observed (Fig. 5C). Next, to validate if changes in mRNA levels translated to proteins, we performed Western blotting using whole cell lysates. Although no differences were observed for K-cadherin levels among the groups (Fig. 5D), significantly reduced expression of OB-cadherin (-2.5-fold, $P < 0.01$) was observed in hTM cells seeded on 10% XCDM compared with uncrosslinked control CDM or 1% XCDM (Fig. 5E).

Ten Percent XCDM Markedly Retained TAZ in the Cytoplasm of hTM Cells

There is mounting evidence Wnt/β-catenin and YAP/TAZ signaling pathways are both involved in mechanotransduction[34,35] and could be functionally linked particularly via TAZ expression/subcellular localization.[39–41] Thus, we subsequently determined the effect of XCDMs on the protein expression of TAZ in hTM cells cultured on CDM and XCDMs in serum-free media for 24 hours using whole cell lysates and nuclear/cytoplasmic fractions. For whole cell lysates, compared with vehicle CDM, 1%, 2%, and 10% XCDMs significantly overexpressed TAZ (1.8-fold, $P < 0.05$; 1.8-fold, $P < 0.05$; and 2.0-fold, $P < 0.01$, respectively) in hTM cells (Fig. 6A). However, only 10% XCDM significantly decreased phosphorylated TAZ (pTAZ; -2-fold, $P < 0.001$) in hTM cells compared with uncrosslinked CDM (Fig. 6B); suggesting TAZ may be active. Further, whereas subcellular fractionation revealed 2% and 10% XCDMs profoundly increased cytoplasmic TAZ (1.9-fold and 2.1-fold, $P < 0.01$, respectively) in hTM cells compared with CDM, there were no significant differences in nuclear TAZ levels among groups (Fig. 6C).

Investigative Ophthalmology & Visual Science

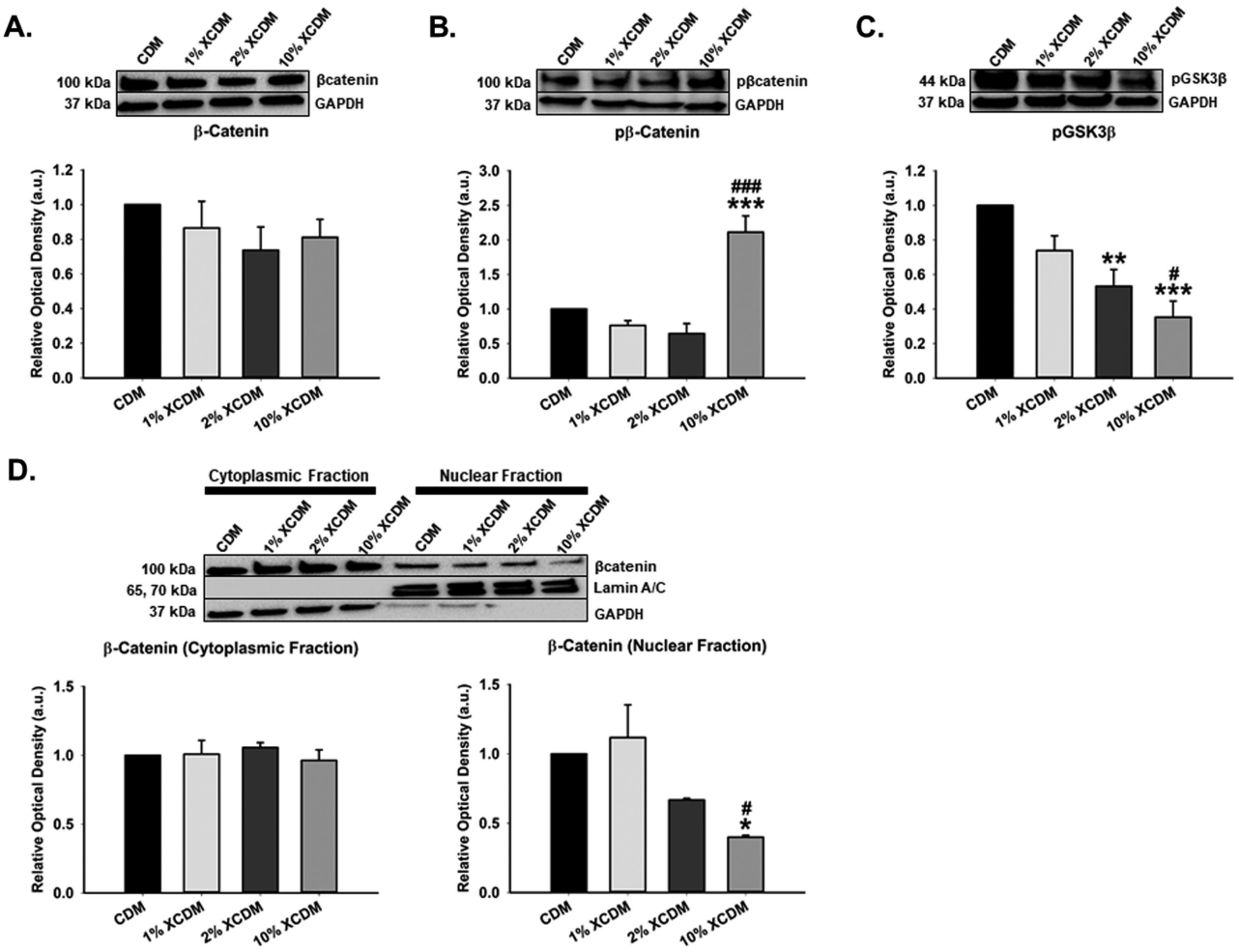

Figure 4. Ten percent (10%) XCDM dysregulated nucleocytoplasmic translocation of β-catenin in hTM cells. Cell-derived matrices (CDMs) were obtained from hTM cells cultured for 4 weeks in complete growth media using 20 mM ammonium hydroxide decellularization buffer. Then, CDMs were crosslinked with vehicle control or 1%, 2%, and 10% genipin/PBS for 5 hours to generate vehicle control (CDM), 1%, 2%, and 10% genipin-induced crosslinked CDMs (1%, 2%, and 10% XCDMs) respectively. New hTM cells of low passage from the same donor used to generate decellularized CDMs were cultured on uncrosslinked CDM and XCDMs in serum-free media for 24 hours. Protein was extracted from whole cell lysates or nuclear/cytoplasmic fractions for Western blot analysis. GAPDH was used as an internal control for normalization. Representative blot (top) and densitometric analysis (bottom) of (**A**) β-catenin, (**B**) phosphorylated β-catenin (pβ-catenin), (**C**) phosphorylated glycogen synthase kinase-3 beta (pGSK3β), (**D**) cytoplasmic and nuclear localization of β-catenin. *Columns and error bars*; means and standard error of mean (SEM). One-way ANOVA with the Tukey pairwise comparisons post hoc test was used for statistical analysis (n =4 biological replicates). $^{*}P < 0.05$, $^{**}P < 0.01$, $^{***}P < 0.001$ for the group of interest versus control, CDM. $^{\#}P < 0.05$, $^{\#\#\#}P < 0.001$ for the group of interest versus 1% XCDM). GAPDH, glyceraldehyde 3-phosphate dehydrogenase; hTM, human trabecular meshwork; PBS, phosphate buffered saline.

Ten Percent XCDM Downregulated Nuclear YAP Levels in hTM Cells Associated with Inactive RhoA/ROCK Signaling Axis

Given that the functions of YAP and TAZ are not necessarily interchangeable,[45,46,72] we proceeded to determine the protein expression levels of YAP in hTM cells seeded on CDM and XCDMs for 24 hours in serum-free media. For whole cell lysates, compared with uncrosslinked CDM, 2% and 10% XCDMs markedly overexpressed YAP (2.2-fold, $P < 0.05$; and 2.9-fold, $P < 0.001$, respectively) in hTM cells (Fig. 7A). Further, there were no significant differences in the expression of phosphorylated YAP (pYAP) in hTM cells on CDM and XCDMs (Fig. 7B). Conversely, nuclear/cytoplasmic fractionation revealed complete translocation of YAP into the nucleus of hTM cells seeded on CDM and XCDMs. Although, in the nucleus, compared with uncrosslinked CDM, whereas 1% XCDM markedly increased YAP (1.4-fold, $P < 0.05$) in hTM cells, 10% XCDM significantly downregulated its expression (-2.5-fold, $P < 0.01$; Fig. 7C). Further, given the role of ras homolog family member a (RhoA)/rho-associated coiled-coil protein kinase (ROCK) signaling axis in the conventional mechanotransduction of YAP and/or TAZ in response to biomechanical cues,[34] we determined the effect of 10% XCDM on the protein expression of RhoA and ROCK in hTM cells after 24 hours. Compared with CDM, 10% XCDM significantly downregulated RhoA (-2.5-fold, $P < 0.001$; Fig. 7D), with no significant change in its downstream kinase, ROCK (Fig. 7E).

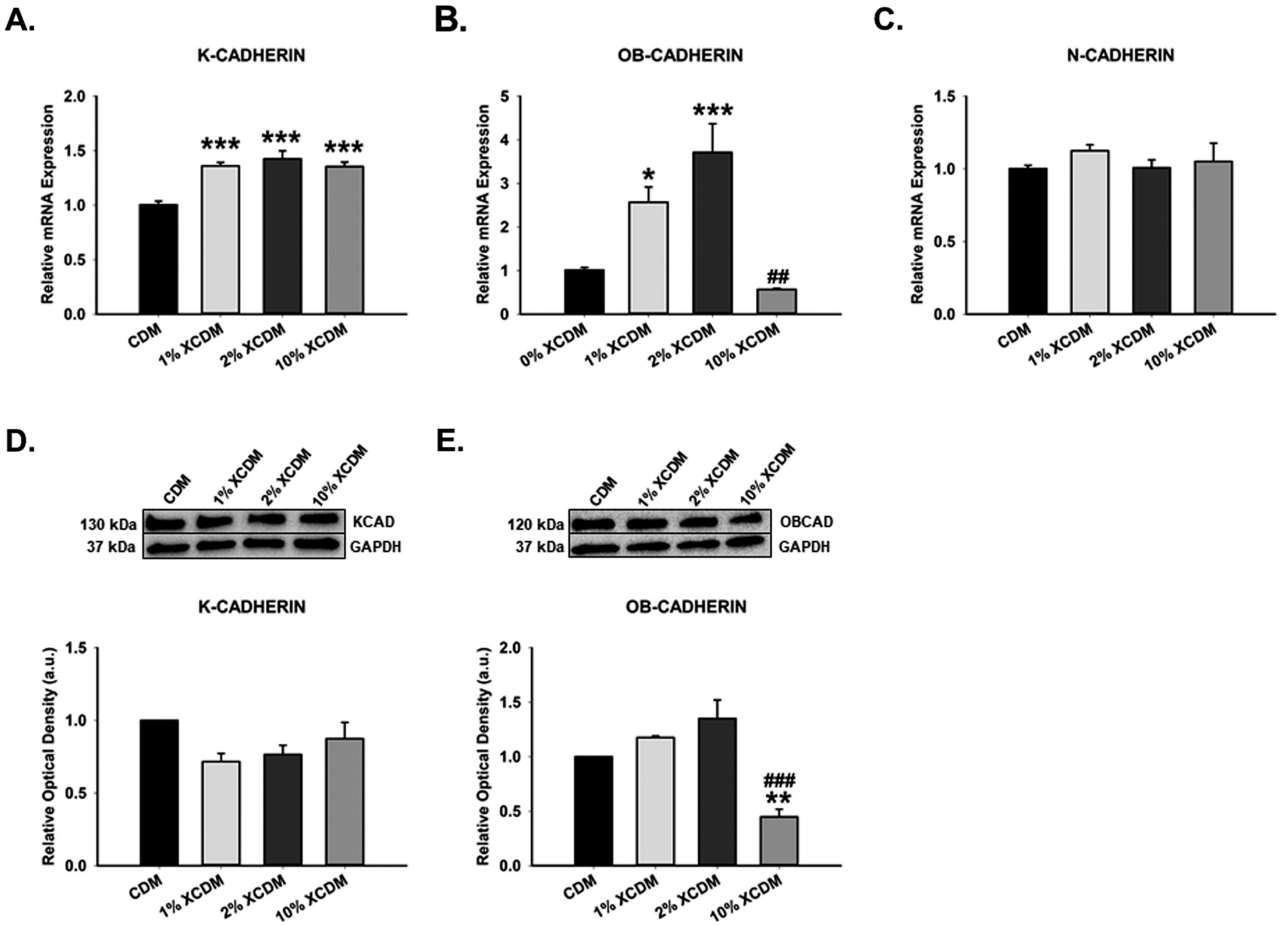

Figure 5. Ten percent (10%) XCDM decreased OB-cadherin protein in hTM cells. 20 mM Ammonium hydroxide decellularization buffer was used to generate cell-derived matrices (CDMs) from primary hTM cells cultured for 4 weeks in complete growth media. After using enzymes to subsequently remove any remaining DNA/RNA, CDMs were treated with vehicle control, 1%, 2%, or 10% genipin/PBS for 5 hours to obtain vehicle control (CDM), 1%, 2%, and 10% genipin-induced crosslinked CDMs (1%, 2%, and 10% XCDMs), respectively. New, low passage, hTM cells from the same donor used to obtain CDMs were seeded on uncrosslinked CDM and XCDMs in serum-free media for 24 hours. RNA was extracted for reverse transcription and qPCR. GAPDH was used as an internal control for normalization. Respective bar graph for the gene expression of (**A**) K-cadherin, (**B**) OB-cadherin, and (**C**) N-cadherin. Further, protein was extracted for Western blot analysis. GAPDH was used as a housekeeping protein for normalization. Representative blot (top) and densitometric analysis (bottom) of (**D**) K-cadherin, and (**E**) OB-cadherin. *Columns and error bars*; means and standard error of mean (SEM). One-way ANOVA with the Tukey pairwise comparisons post hoc test was used for statistical analysis (n =3 biological replicates for gene expression data and 4 biological replicates for protein expression data. $^{*}P < 0.05$, $^{**}P < 0.01$, $^{***}P < 0.001$ for the group of interest versus control, CDM. $^{\#\#}P < 0.01$, $^{\#\#\#}P < 0.001$ for the group of interest versus 1% XCDM). GAPDH, glyceraldehyde 3-phosphate dehydrogenase; hTM, human trabecular meshwork; PBS, phosphate buffered saline.

Ten Percent XCDM Profoundly Downregulated Key Target Genes of β-Catenin and YAP/TAZ Signaling Pathways

In order to confirm the resultant effect of XCDMs on β-catenin and YAP/TAZ signaling pathways in hTM cells, we subsequently quantitated the transcriptional expression of key target genes of these signaling pathways. We extracted RNA from hTM cells cultured on CDM or 1%, 2%, and 10% XCDMs for 24 hours in serum-free media and performed qPCR. Compared with uncrosslinked CDM, 2% and 10% XCDM significantly downregulated Axin2 gene (-1.4-fold and -2-fold, $P < 0.001$, respectively) in hTM cells (Fig. 8A). Additionally, compared with CDM, whereas 1% XCDM increased subtly, yet significantly, the gene expression of CD44 (1.2-fold, $P < 0.05$) in hTM cells, 2% and 10% XCDMs markedly decreased its expression (-1.4- and -2-fold, $P < 0.001$, respectively; Fig. 8B). Compared with cells on uncrosslinked control CDMs, hTM cells cultured on 2% and 10% XCDMs had marked reductions in connective tissue growth factor gene (CTGF; -1.4- and -2-fold, $P < 0.001$, respectively; Fig. 8C). Further, whereas 1% XCDM significantly increased levels of caveolin 1 gene (1.3-fold, $P < 0.01$), 10% XCDM markedly reduced its expression (-1.3-fold, $P < 0.05$) in hTM cells compared with uncrosslinked control CDM (Fig. 8D). Moreover, compared with cells on CDM, hTM cells on 2% and 10% XCDMs had cavin1 gene downregulated (-1.7-fold and -3.3-fold, $P < 0.001$, respectively; Fig. 8E). Finally, only 10% XCDM significantly reduced levels of actin alpha 2 (ACTA2) smooth muscle gene (-2-fold, $P < 0.01$) in hTM cells compared with uncrosslinked CDM (Fig. 8F).

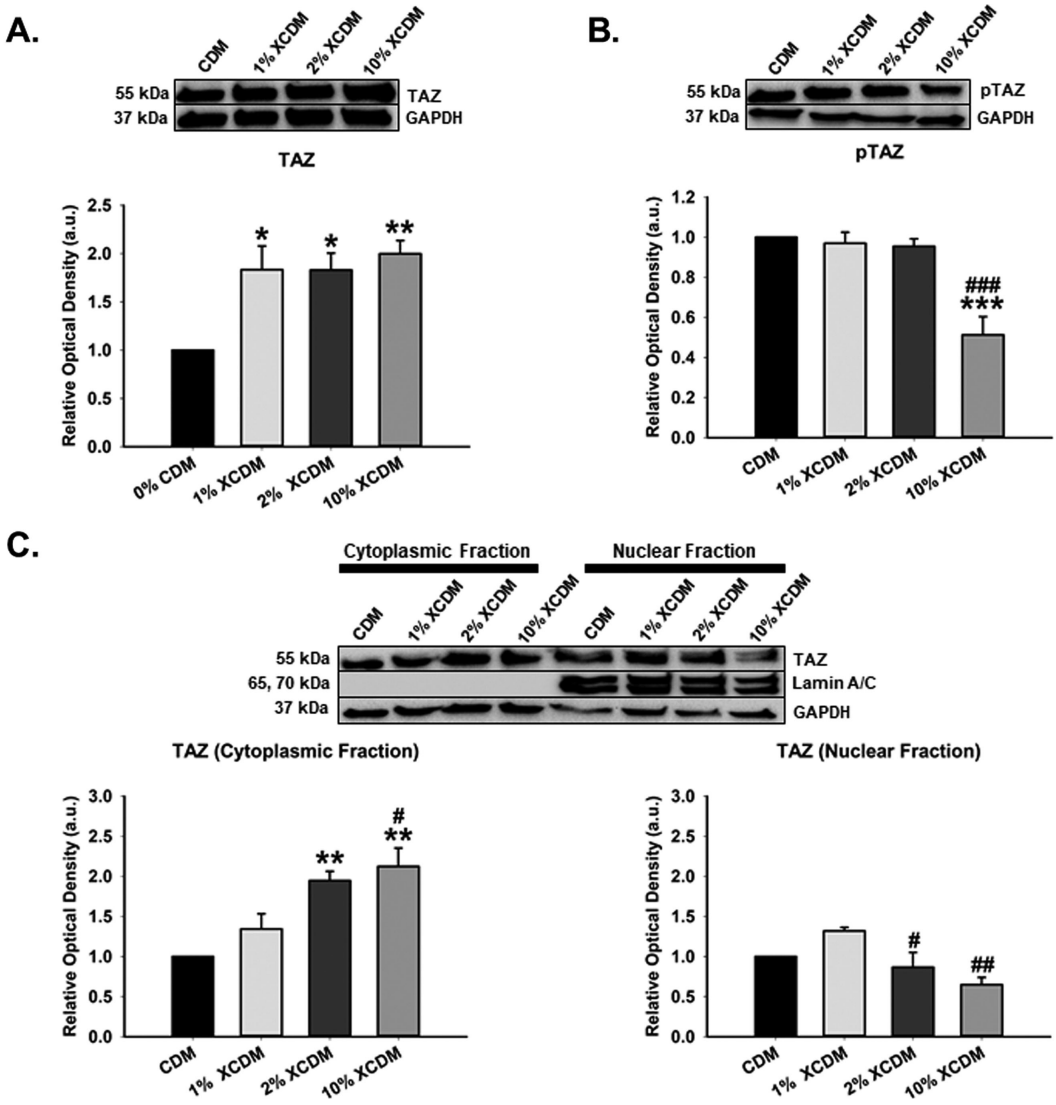

Figure 6. Ten percent (10%) XCDM markedly retained TAZ in the cytoplasm of hTM cells. Cell-derived matrices (CDMs) were generated from hTM cells cultured for 4 weeks in complete growth media using 20 mM ammonium hydroxide decellularization buffer. Afterward, CDMs were crosslinked with vehicle control or 1%, 2%, and 10% genipin/PBS for 5 hours to derive vehicle control (CDM), 1%, 2%, and 10% genipin-induced crosslinked CDMs (1%, 2%, and 10% XCDMs), respectively. New, low passage, hTM cells from the same donor used to obtain decellularized CDMs were seeded on uncrosslinked control CDM and XCDMs in serum-free media for 24 hours. Protein was extracted from whole cell lysates or subcellular fractions for Western blot analysis. GAPDH was used as an internal control for normalization. Representative blot (top) and densitometric analysis (bottom) of (**A**) transcriptional coactivator with PDZ-binding motif (TAZ), (**B**) phosphorylated TAZ (pTAZ), and (**C**) cytoplasmic and nuclear localization of TAZ. *Columns and error bars*; means and standard error of mean (SEM). One-way ANOVA with the Tukey pairwise comparisons post hoc test was used for statistical analysis (n =4 biological replicates. $^{*}P < 0.05$, $^{**}P < 0.01$, $^{***}P < 0.001$ for the group of interest versus control, CDM. $^{\#}P < 0.05$, $^{\#\#}P < 0.01$, $^{\#\#\#}P < 0.001$ for the group of interest versus 1% XCDM). GAPDH, glyceraldehyde 3-phosphate dehydrogenase; hTM, human trabecular meshwork; PBS, phosphate buffered saline.

Ten Percent XCDM Markedly Decreased Critical Target Proteins of β-Catenin and YAP/TAZ Signaling Pathways

Next, we determined the effect of uncrosslinked control CDM and 10% XCDM on the protein expression of few targets of Wnt/β-catenin and YAP/TAZ signaling pathways in hTM cells after 24 hours. We restricted our comparisons to CDM and 10% XCDM because the latter had the greatest adverse effect on β-catenin and YAP/TAZ signaling. We found that, compared with uncrosslinked control CDM, CTGF was significantly decreased by 10% XCDMs (-2.5-fold, $P < 0.001$) in hTM cells (Fig. 9A). Similarly, compared with vehicle CDM, 10% XCDM markedly downregulated total fibronectin (-2.5-fold, $P < 0.001$), fibronectin extra-domain A (EDA) isoform (-100-fold, $P < 0.001$) and α-smooth muscle actin (αSMA; -1.4-fold, $P < 0.001$; Figs. 9B, 9C, 9D) in hTM cells.

Wnt/β-Catenin Activation Rescued hTM Cells from 10% XCDM-Induced Stiffening Associated with Increased Nuclear β-Catenin Levels

Finally, because inhibition of Wnt/β-catenin signaling pathway is associated with stiffening of hTM cells cultured on plastic substrates,[50] we determined whether activation of this pathway could rescue hTM cells from 10% XCDM-

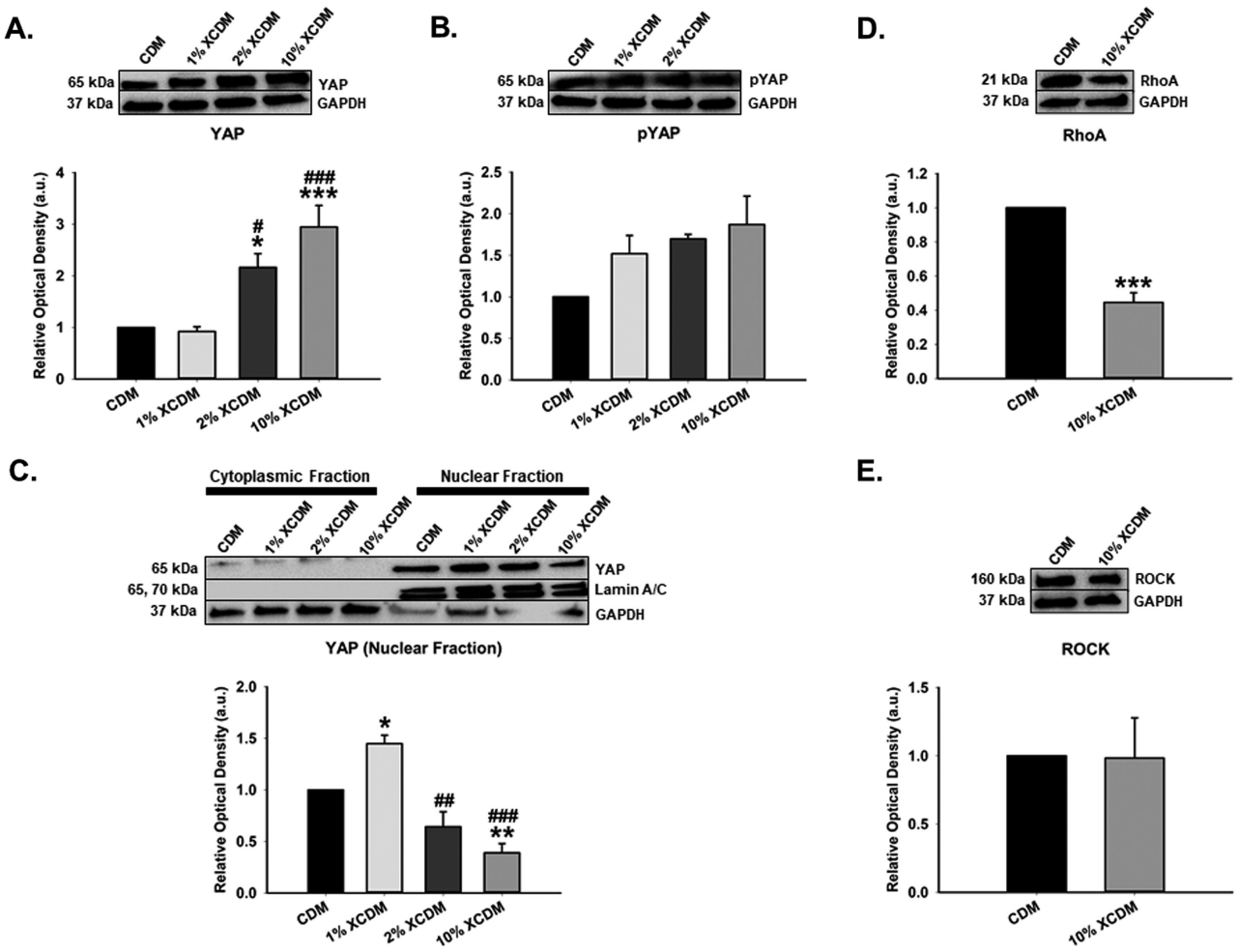

Figure 7. Ten percent (10%) XCDM induced low nuclear YAP levels together with inactivation of RhoA/ROCK signaling axis in hTM cells. The 20 mM ammonium hydroxide decellularization buffer was used to generate cell-derived matrices (CDMs) from primary hTM cells following 4 weeks of culturing in complete growth media. Next, decellularized CDMs were crosslinked with vehicle control or 1%, 2%, and 10% genipin/PBS for 5 hours to obtain vehicle control (CDM), 1%, 2%, and 10% genipin-induced crosslinked CDMs (1%, 2%, and 10% XCDMs) respectively. New hTM cells of low passage from the same donor utilized to generate CDMs were cultured on uncrosslinked CDM and XCDMs in serum-free media for 24 hours. Protein was extracted from whole cell lysates or nuclear/cytoplasmic fractions for Western blot analysis. GAPDH was used a housekeeping protein for normalization. Representative blot (top) and densitometric analysis (bottom) of (**A**) Yes-associated protein (YAP), (**B**) phosphorylated YAP (pYAP), (**C**) cytoplasmic and nuclear localization of YAP, (**D**) Ras homolog family member A (RhoA), and (**E**) Rho-associated coiled-coil-containing protein kinases (ROCK). *Columns and error bars*; means and standard error of mean (SEM). One-way ANOVA with the Tukey pairwise comparisons post hoc test was used for statistical analysis for **A**, **B**, and **C** whereas unpaired Student's *t*-test was used for statistical analysis of **D** and **E** (n =4 biological replicates. $^{*}P < 0.05$, $^{**}P < 0.01$, $^{***}P < 0.001$ for the group of interest versus control, CDM. $^{\#}P < 0.05$, $^{\#\#}P < 0.01$, $^{\#\#\#}P < 0.001$ for the group of interest versus 1% XCDM). GAPDH, glyceraldehyde 3-phosphate dehydrogenase; hTM, human trabecular meshwork; PBS, phosphate buffered saline.

induced stiffening. We subsequently determined the elastic moduli of hTM cells seeded on uncrosslinked control CDM or 10% XCDM with or without 250 nM canonical Wnt/β-catenin pathway activator (LY2090314) in serum-free media for 24 hours. We observed that Wnt pathway activation rescued hTM cells from 10% XCDM-induced stiffening, with an elastic modulus similar to that of cells cultured on uncrosslinked control CDMs (Fig. 10A). In parallel experiments, we quantified subcellular localization of β-catenin in hTM cells cultured on CDM or 10% XCDM, and with or without 250 nM Wnt activator, or 10 µM Wnt inhibitor (LGK974), in serum-free media for 24 hours. The Wnt inhibitor was used as a negative control for the activator (LY2090314) to confirm that Wnt inhibition indeed results in lesser nuclear β-catenin. Compared with uncrosslinked control CDM, whereas 10% XCDM alone did not alter cytoplasmic β-catenin levels, its expression was significantly downregulated in hTM cells by either 10% XCDM-Wnt activator interaction (-2.5-fold, $P < 0.01$) or 10% XCDM-Wnt inhibitor interaction (-1.7-fold, $P < 0.05$). Concurrently, compared with vehicle CDM, whereas 10% XCDM markedly reduced β-catenin levels in the nucleus of hTM cells with (-1.7-fold, $P < 0.001$) or without (-3.3-fold, $P < 0.001$) the Wnt inhibitor, it significantly elevated nuclear β-catenin levels (1.5-fold, $P < 0.001$) with Wnt activation (Figs. 10B 10C).

Discussion

Genipin-Induced Crosslinked CDM Alters Cellular Biomechanics

Increased TM ECM crosslinking and stiffness have been implicated in ocular hypertension and glaucoma.[15,19,21,23–26]

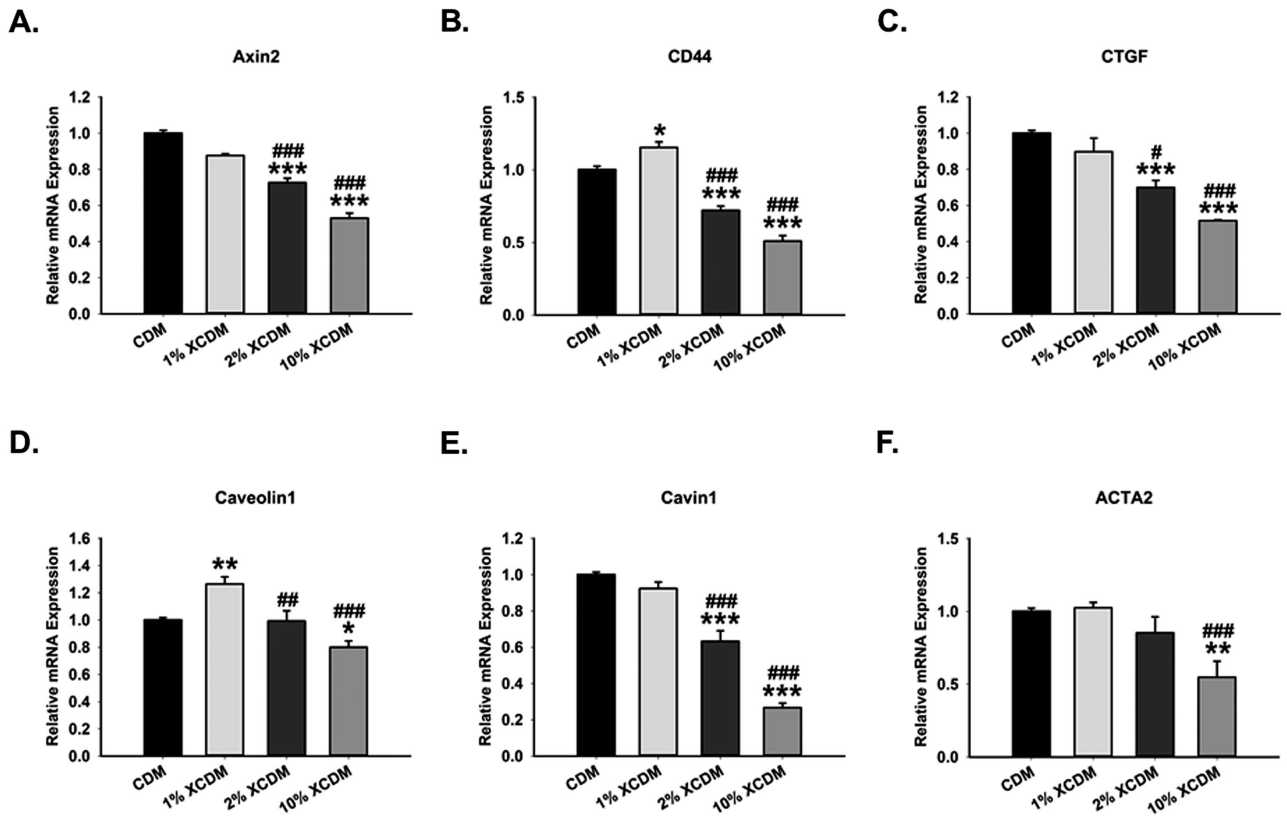

Figure 8. Ten percent (10%) XCDM markedly decreased key target genes of β-catenin and YAP/TAZ signaling pathways. Cell-derived matrices (CDMs) were generated from hTM cells cultured for 4 weeks in complete growth media using 20 mM ammonium hydroxide decellularization buffer. Then, CDMs were crosslinked with vehicle control or 1%, 2%, and 10% genipin/PBS for 5 hours to obtain vehicle control (CDM), 1%, 2%, and 10% genipin-induced crosslinked CDMs (1%, 2%, and 10% XCDMs), respectively. New hTM cells of low passage from the same donor used to derive CDMs were cultured on uncrosslinked control CDM and XCDMs in serum-free media for 24 hours. RNA was extracted for reverse transcription and qPCR. GAPDH was used as a housekeeping gene for normalization. Respective bar graph for the gene expression of (**A**) Axin2, (**B**) CD44, (**C**) connective tissue growth factor (CTGF), (**D**) Caveolin1, (**E**) Cavin1, and (**F**) Actin alpha 2 (ACTA2). *Columns and error bars*; means and standard error of mean (SEM). One-way ANOVA with the Tukey pairwise comparisons post hoc test was used for statistical analysis (n =3 biological replicates. $^{*}P < 0.05$, $^{**}P < 0.01$, $^{***}P < 0.001$ for the group of interest versus control, CDM. $^{\#}P < 0.05$, $^{\#\#}P < 0.01$, $^{\#\#\#}P < 0.001$ for the group of interest versus 1% XCDM). GAPDH, glyceraldehyde 3-phosphate dehydrogenase; hTM, human trabecular meshwork; PBS, phosphate buffered saline.

However, whether a crosslinked TM ECM is capable of precipitating profibrotic phenotypes (for example, cell stiffening) and/or dysregulating key mechanotransduction pathways in hTM cells remain(s) unknown. Using genipin, a natural collagen crosslinker, we generated and characterized matrices of varying stiffness, documented their effect on cellular biomechanics, together with their simultaneous impact on two mechanotransduction pathways (Wnt/β-catenin and YAP/TAZ) implicated in ocular hypertension/glaucoma. As expected, genipin potently induced ECM crosslinks, in a concentration dependent manner, as evidenced by increased GGEL immunolabeling, multiple overlaps between major structural ECM proteins and a "fused" morphology. This was accompanied by increases in matrix stiffness with the greatest effect observed with 10% XCDM. The concentration of genipin used to generate 10% XCDM is similar to that utilized by Yang and colleagues (i.e. 22 μM),[25] which resulted in a reduction of outflow facility in porcine eyes ex vivo. Such a reduction in facility represents loss of outflow homeostasis congruent with what is observed in human glaucomatous eyes.[61]

Having confirmed that genipin potently stiffens the matrix, we next demonstrated that hTM cells cultured on these crosslinked matrices have greater elastic moduli. That both 2% and 10% XCDMs profoundly stiffened hTM cells is consistent with the observation that cells on stiffer substrates are stiffer. Previous studies,[34,67,73–76] including those from our group,[20,61] have implicated substratum properties in influencing cellular biomechanics. Given the relationship between increased stiffness and ocular hypertension,[19] XCDM-induced cell stiffening may play a determining role in how increased TM ECM crosslinking reduces outflow facility ex vivo or causes ocular hypertension in vivo.[23–25] Nevertheless, further investigations are required to determine if these stiffer cells are capable of exerting greater forces on the crosslinked CDMs, and what the specific causes of such stiffening may be. For instance, where the cause is due to molecular interactions and/or cell adhesion and spreading, or alternatively, due to morphological cues which guide the stiffening remain to be seem.

Genipin-Induced Crosslinked CDM Modulates the Wnt/β-Catenin Pathway

Because Wnt is a critical signaling pathway implicated in mechanotransduction,[35,37] TM dysfunction,[49,50] and ocular hypertension,[51] we next investigated if this pathway is

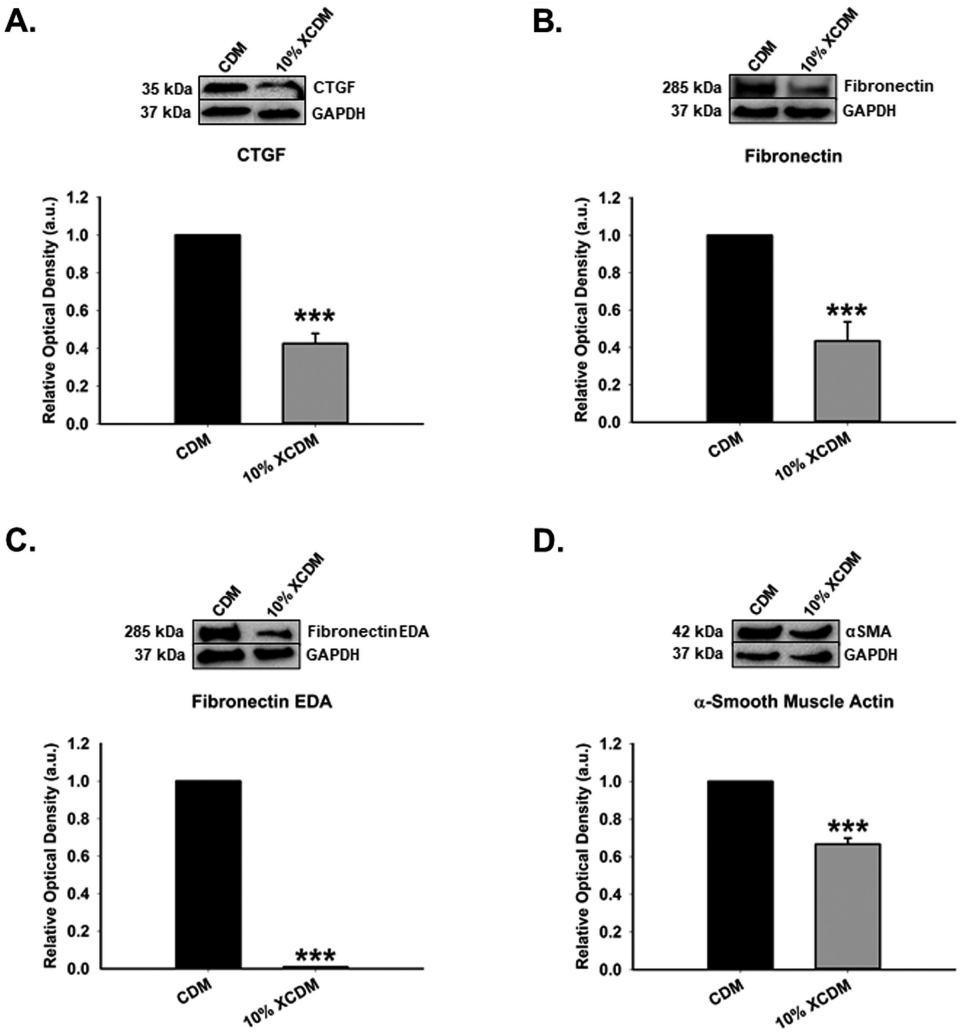

Figure 9. Ten percent (10%) XCDM downregulated crucial target proteins of β-catenin and YAP/TAZ signaling pathways. 20 mM Ammonium hydroxide decellularization buffer was used to generate cell-derived matrices (CDMs) from primary hTM cells following 4 weeks of culturing in complete growth media. Subsequently, CDMs were crosslinked with vehicle control or 10% genipin/PBS for 5 hours to obtain vehicle control (CDM) and 10% genipin-induced crosslinked CDMs (10% XCDMs), respectively. New, low passage, hTM cells from the same donor used to generate CDMs were cultured on uncrosslinked control CDM and XCDMs in serum-free media for 24 hours. Protein was extracted for Western blot analysis. GAPDH was used an internal control for normalization. Representative blot (top) and densitometric analysis (bottom) of (**A**) connective tissue growth factor (CTGF), (**B**) fibronectin, (**C**) fibronectin extra-domain A (EDA) isoform, and (**D**) α-smooth muscle actin (αSMA). *Columns and error bars*; means and standard error of mean (SEM). Unpaired Student's *t*-test was used for statistical analysis ($n = 4$ biological replicates. $^{***}P < 0.001$ for 10% XCDM versus uncrosslinked control, CDM). GAPDH, glyceraldehyde 3-phosphate dehydrogenase; hTM, human trabecular meshwork; PBS, phosphate buffered saline.

modulated in hTM cells cultured on crosslinked CDMs. We observed cytoplasmic retention of inactive β-catenin (given increased pβ-catenin and reduced pGSK3β) in hTM cells cultured on 10% XCDM, suggesting the Wnt/β-catenin pathway may be inhibited. That cytoplasmic retention of β-catenin is marked for degradation by the cytosolic multiprotein complex to inhibit the canonical Wnt/β-catenin pathway is documented.[71,77] Correspondingly, in hTM cells cultured on 10% XCDM, at an early time point (24 hours), we observed reduced expression of critical target genes and proteins of Wnt/β-catenin pathway like Axin2, CD44, total fibronectin, and fibronectin EDA isoform. Whereas Wnt antagonism has been shown to be implicated in POAG, elevated intraocular pressure,[49] and cell stiffening,[50] activation of this pathway may have a therapeutic benefit by inhibiting transforming growth factor beta 2 (TGFβ2) signaling pathway,[69] a well-established profibrotic pathway in POAG,[78,79] reducing the expression of profibrotic ECM proteins,[70,80] and/or regulating cell-cell contacts via K-cadherin expression.[51] Regarding the latter, cadherins' role in maintaining cell-cell adhesion is partly to allow for their mechanosensitive/mechanotransduction function,[81–83] together with formation of gap junctions to enhance cell-cell communication.[84,85] Thus, downregulation of OB-cadherin in hTM cells on 10% XCDM in this study may suggest OB-cadherin-dependent mechanotransduction has gone awry and/or paracrine cell signaling is impaired. Webber and colleagues[51] implicated K-cadherin's expression as an important aspect of how active Wnt/β-catenin signaling maintains aqueous homeostasis in mice and hTM

Investigative Ophthalmology & Visual Science

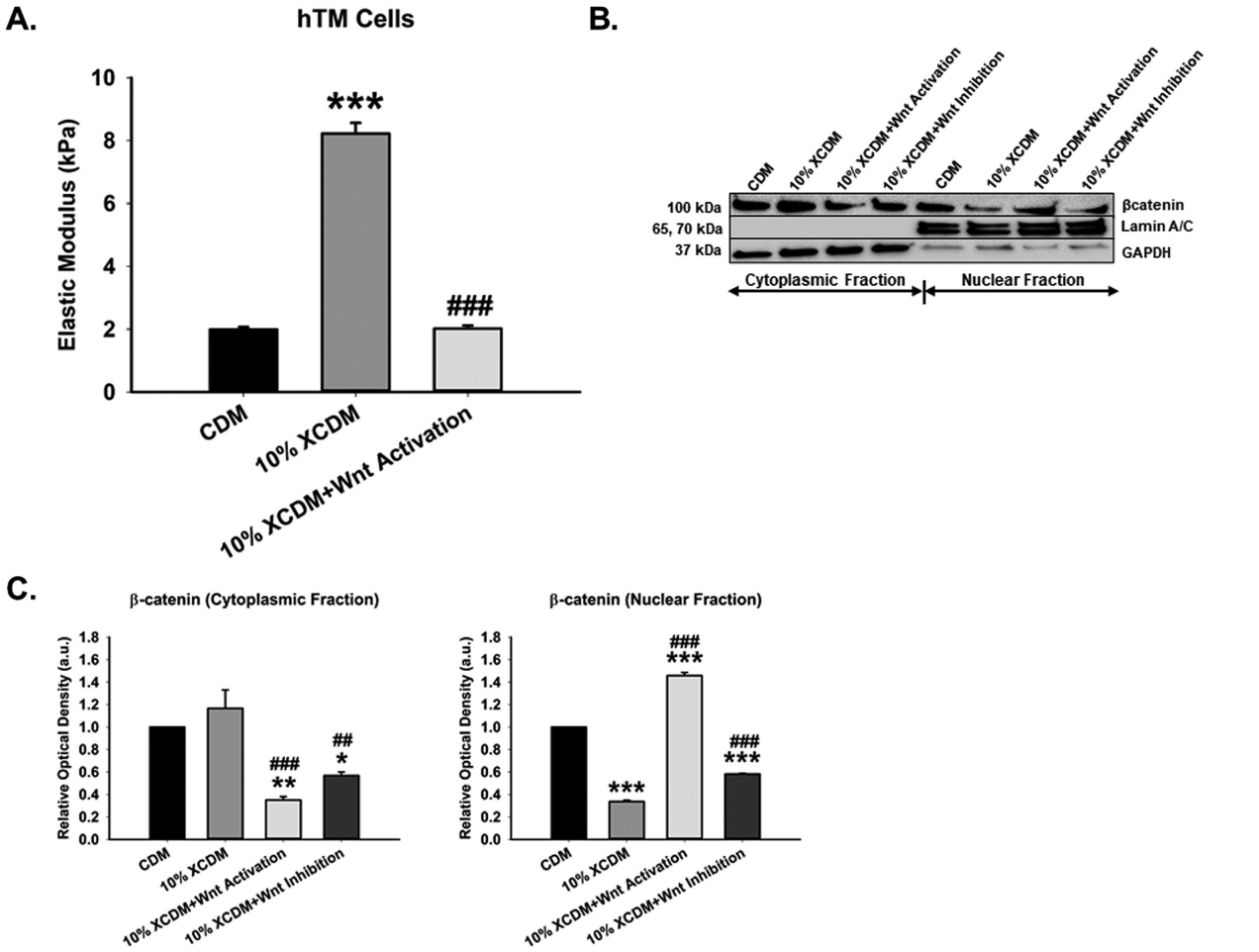

Figure 10. Activation of Wnt/β-catenin signaling pathway rescued hTM cells from 10% XCDM-induced stiffening associated with increased nuclear β-catenin levels. Cell-derived matrices (CDMs) were generated from hTM cells cultured for 4 weeks in complete growth media using 20 mM ammonium hydroxide decellularization buffer. Subsequently, CDMs were crosslinked with vehicle control or 10% genipin/PBS for 5 hours to derive vehicle control (CDM) and 10% genipin-induced crosslinked CDMs (10% XCDM), respectively. For cell mechanics, new hTM cells of low passage from the same donor used to derive CDMs were seeded on vehicle control CDM and 10% XCDM in the presence or absence of 250 nM Wnt signaling activator (LY2090314) in serum-free media for 24 hours. Subsequently, atomic force microscopy using normal PNP-TR cantilevers with conical tips was performed. At least 5 measurements were taken for any random cell; with a total of 10 cells probed for each experimental sample. Bar graph shows (**A**) elastic moduli of hTM cells seeded on CDM, 10% XCDM, and 10% XCDM+ Wnt activator. Further, for protein expression, new, low passage, hTM cells were seeded on CDM and 10% XCDM in the presence or absence of 250 nM Wnt signaling activator (LY2090314) or 10 µM Wnt inhibitor (LGK974) in serum-free media for 24 hours. Protein was extracted from nuclear/cytoplasmic fractions for Western blot analysis. GAPDH was used as a housekeeping protein for normalization. (**B**) Representative blot and (**C**) densitometric analysis of cytoplasmic and nuclear localization of β-catenin. *Columns and error bars*; means and standard error of mean (SEM). One-way ANOVA with the Tukey pairwise comparisons post hoc test was used for statistical analysis (n =4 biological replicates. $^{*}P < 0.05$, $^{**}P < 0.01$, $^{***}P < 0.001$ for the group of interest versus control, CDM. $^{\#\#}P < 0.01$, $^{\#\#\#}P < 0.001$ for the group of interest versus 10% XCDM). GAPDH, glyceraldehyde 3-phosphate dehydrogenase; hTM, human trabecular meshwork; PBS, phosphate buffered saline.

cells. Therefore, in this study, with 10% XCDM-induced inactivated Wnt/β-catenin pathway, we should have seen a corresponding decrease in the protein expression of K-cadherin in hTM cells. Instead, OB-cadherin protein was downregulated suggesting that regulation of specific cadherins by Wnt/β-catenin pathway at least at the protein level may be ligand-specific (crosslinked TM CDMs in ours versus chemical Wnt activators/inhibitors in theirs). Further studies with subcellular fractionation (for example, plasma membrane fraction versus whole cells) are required to establish the precise relationship between crosslinked CDM-mediated modulation of Wnt/β-catenin pathway and cadherins in hTM cells.

Genipin-Induced Crosslinked CDM Dysregulates the YAP/TAZ Pathway

Intersecting the Wnt/β-catenin signaling pathway are YAP and TAZ,[38–44] whose mechanotransduction function conventionally involves their subsequent nuclear translocation, following activation of the actin cytoskeleton or actomyosin machinery.[34,52,80] Several studies have reported inhibitory crosstalk between canonical Wnt/β-catenin and Hippo/YAP/TAZ pathways in non-ocular cells/tissues, in response to chemical ligands. In these previous studies, YAP/TAZ pathway inhibited the Wnt pathway via the following mechanisms: (i) direct binding of Hippo-induced

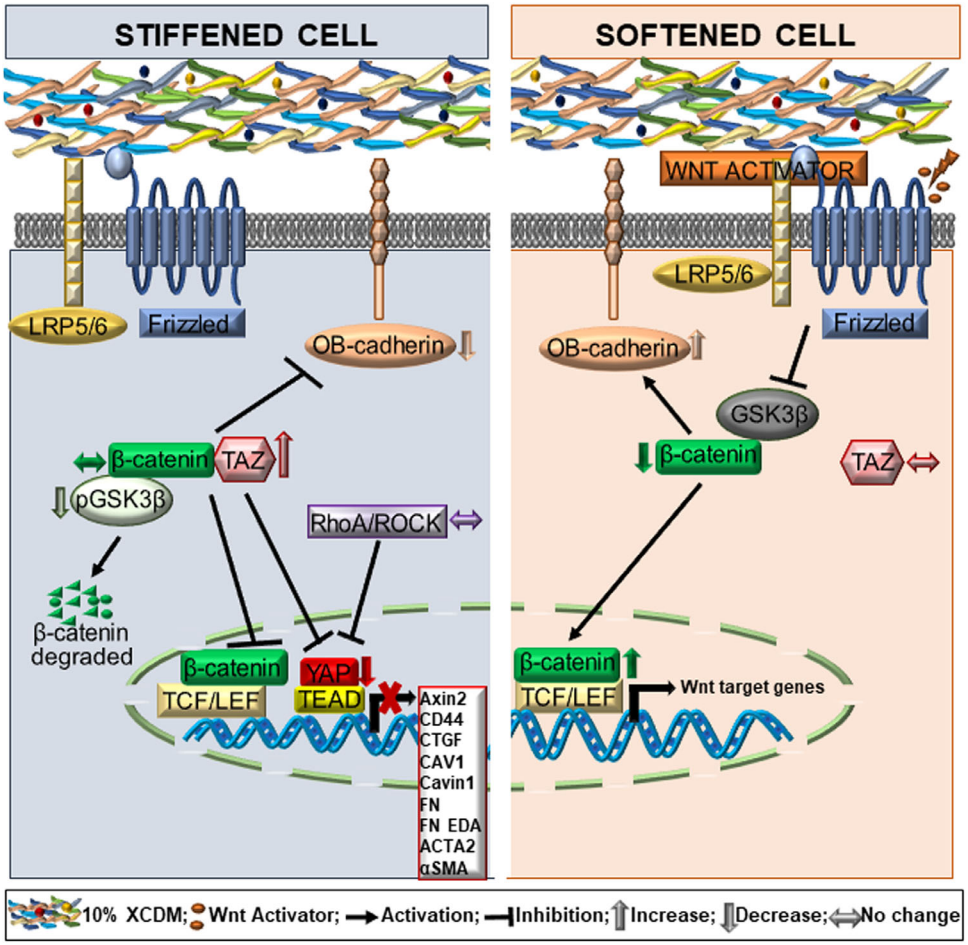

Figure 11. Proposed mechanisms associated with 10% XCDM-induced hTM cell stiffening and Wnt pathway activation-mediated rescue of cells from stiffening. (Left cellular compartment) Ten percent (10%) XCDM-induced cell stiffening is associated with increased active cytoplasmic TAZ, which may adversely interact with cytoplasmic β-catenin, thereby dysregulating the latter's nuclear shuttling and/or its regulation of OB-cadherin, important for maintaining aqueous homeostasis. Decreased pGSK3β suggests probable subsequent degradation of cytoplasmic β-catenin. Further, elevated active cytoplasmic TAZ may directly prevent interaction of nuclear YAP with TEAD, and this may worsen with no ROCK activity. Consequently, suppression of key target genes and proteins of Wnt/β-catenin and YAP/TAZ pathways ensue, suggesting 10% XCDM stiffens hTM cells by dysregulating these two major mechanotransduction pathways. (Right cellular compartment) Activating the Wnt pathway via inhibiting GSK3β may shield β-catenin from cytoplasmic TAZ's inhibition, increase nuclear levels of β-catenin to activate Wnt target gene expression in rescuing hTM cells from 10% XCDM-induced stiffening. Further, activation of the Wnt pathway may enhance β-catenin-dependent increase of OB-cadherin in regulating cell-cell contacts important for aqueous homeostasis. 10% XCDM, 10% genipin-induced crosslinked trabecular meshwork cell-derived matrix; ACTA2, actin alpha 2; αSMA, α-smooth muscle actin; CAV1, caveolin1; CD44, cluster of differentiation 44; CTGF, connective tissue growth factor; FN, fibronectin; FN EDA, fibronectin extra-domain A isoform; GSK3β, glycogen synthase kinase-3 beta; LEF, lymphoid enhancer-binding factor; LRP5/6, lipoprotein receptor-related protein 5/6; pGSK3β, phosphorylated GSK3β; RhoA, Ras homolog family member A; ROCK, Rho-associated coiled-coil protein kinase; TAZ, transcriptional coactivator with a PDZ-binding motif; TCF, T-cell factor; TEAD, transcriptional enhancer factor-domain; YAP, Yes-associated protein.

inactivated YAP or TAZ to either β-catenin or disheveled in the cytoplasm,[38,39] (ii) prevention of β-catenin' nuclear translocation,[38] (iii) direct binding between YAP and β-catenin in the nucleus,[43] and/or (iv) RhoA/ROCK-mediated activation of YAP/TAZ to promote expression of Wnt antagonists.[42] In this study, we show that 10% XCDM-induced inactivation of the Wnt pathway in hTM cells was associated with concurrent retainment of an increased expression of TAZ (likely active given downregulation of pTAZ) in the cytoplasm, reduced expression of YAP in the nucleus, together with no difference in RhoA/ROCK expression. Consequently, key target genes and proteins of the YAP/TAZ pathway like CTGF, Caveolin1, Cavin1, Acta2, and αSMA were downregulated in hTM cells on 10% XCDM. Our findings suggest several important mechanisms could be at play with regard to the probable roles of YAP and TAZ in XCDM-induced stiffening of hTM cells. First, increased cytoplasmic TAZ may bind to β-catenin and/or disheveled in the cytoplasm to hinder β-catenin's nuclear translocation consistent with previous studies.[38,39] Alternatively, increased cytoplasmic TAZ may negatively regulate expression/activity of YAP in the nucleus in agreement with a previous study from our group in corneal stromal cells,[86] and that of Tang and colleagues,[87] who demonstrated that the transcriptional co-activator functions of YAP and TAZ are inversely regulated by tyrosine phosphorylation status of parafibromin. It

is also likely that 10% XCDM-induced cell stiffening may be independent of the conventional mechanotransduction signaling axis of YAP/TAZ, which typically involves ROCK or actomyosin activity.[34,52] Finally, a reduction in Caveolin1 and Cavin1 may result in loss of and/or defective formation of plasma membrane-bound organelle caveolae, congruent with a previous study,[88] which may impair their homeostatic mechanosensitive function upstream of YAP/TAZ,[89] and subsequently induce stiffening[90] in correlation with ocular hypertension.[91] Further studies are certainly required to disseminate the exact mechanistic interaction between the Wnt/β-catenin and YAP/TAZ signaling pathways in hTM cells cultured on XCDMs.

Canonical Wnt Pathway Activation Rescues hTM Cell Stiffening by XCDM

Finally, because 10% XCDM stiffened hTM cells in correlation with inactivating the Wnt pathway, and antagonism of this pathway had previously been implicated in hTM cell stiffening,[50] we explored whether activation of this pathway could rescue hTM cells from 10% XCDM-induced stiffening. Intriguingly, canonical Wnt pathway activation (via inhibition of GSK3β) abrogated 10% XCDM-dependent stiffening of hTM cells, consistent with a recent study from our group,[80] where canonical Wnt pathway activation reversed the pro-fibrotic effects (for instance, cell stiffening) of Wnt pathway inhibition in hTM cells seeded on glass/plastic substrates.

Limitations

We recognize that this study is not without limitations. First, similar to LOX,[27] genipin crosslinks collagen by forming highly reactive aldehydes on its lysine, hydroxylysine or arginine residues.[53–55] However, apart from structural ECM proteins, it is feasible that genipin may crosslink secreted proteins and/or bioactive peptides in the extracellular milieu, altering the availability/distribution of ligands that cells can interact with. Second, all our end points were determined at 24 hours after plating hTM cells on XCDMs. Whether longer time durations would have resulted in a different pattern of β-catenin and YAP/TAZ localization, ROCK activity and cell stiffness remains to be seen. We recognize that the causal molecules (if any) that may perturb the Wnt/YAP/TAZ pathway(s) in cells cultured on XCDMs were not determined. Further, because no changes in ROCK expression were observed, it is unclear what the specific causes for XCDM-induced cell stiffening may be. Thus, causality-driven investigations implicating mechanosensors, such as integrins, caveolae, or focal adhesion complexes, cell adhesion, cell spreading, geometry, and volume, and other cytoskeletal-related proteins, besides ROCK, in 10% XCDM-induced cell stiffening are warranted.

Summary

In this study, first, we showed that genipin induced matrix stiffening was concentration dependent. Subsequently, we demonstrated that 10% genipin-induced crosslinked cell-derived matrix (10% XCDM) profoundly stiffened hTM cells; and this increased stiffness was associated with dysregulation in nucleocytoplasmic shuttling of β-catenin, reduction of OB-cadherin, retention of TAZ in the cytoplasm (that is likely active), and decreased nuclear YAP levels in hTM cells. Correspondingly, key target gene and protein expressions of Wnt/β-catenin and/or YAP/TAZ pathways in hTM cells were impaired (see Fig. 11, left cellular compartment). Consequently, for the first time, we uncover concurrent dysregulation of two major mechanotransduction pathways, Wnt/β-catenin and YAP/TAZ, associated with cell stiffening by increased ECM crosslinking in hTM cells. We speculate from our findings that these aberrant observations via 10% XCDM in hTM cells are likely due to profound and potent changes in the biochemical, morphological, and biomechanical attributes of the crosslinked ECM. These ECM-derived properties most likely instructed the quality and quantity of extracellular ligands available for interaction with hTM cells via critical mechanosensors. This may explain why 10% XCDM exaggerated responses in hTM cells beyond their homeostatic recovery limits compared with 2% XCDM. Thus, the conditions presented by 10% XCDM mimic a glaucomatous phenotype, thereby providing a model system to investigate the underlying specific causes of the disease especially in the context of aberrant ECM crosslinking. Finally, we demonstrate that in the event of increased TM ECM crosslinking, activation of the Wnt pathway may increase nuclear β-catenin levels and/or cell-cell contacts (see Fig. 11, right cellular compartment), shielding hTM cells from potentially damaging ocular hypertensive phenotypes due to increased stiffness, to maintain their critical homeostatic aqueous drainage functions.

Acknowledgments

The authors thank Alan R. Burns and Sam Hanlon for technical support with scanning electron microscopy, Hasna Baidouri with hTM cell isolation, and their funding sources: startup funding from UHCO (V.K.R.), NIH/NEI grants EY026048-01A1 (J.A.V. and V.K.R.), 5 P30 EY007551-30 (NEI Core grant to UHCO), and P30 EY010572 (NEI Core grant to OHSU), student Vision Research Support Grant (sVRSG), University of Houston College of Optometry (F.Y.), Sigma Xi's Grant in Aid of Research (G2019100198492848; F.Y.), and by an unrestricted grant to the Casey Eye Institute from Research to Prevent Blindness, New York, NY. The authors also thank SavingSight (Kansas City, MO) eye bank for procuring all human donor eyes used in this work. Most importantly, we would like to thank the families of the organ donors without whose consent these experiments would be impossible.

Disclosure: **F. Yemanyi,** None, **J. Vranka,** None; **V.K. Raghunathan,** None

References

1. Quigley HA. Number of people with glaucoma worldwide. *Br J Ophthalmol*. 1996;80:389–393.
2. Kapetanakis VV, Chan MPY, Foster PJ, Cook DG, Owen CG, Rudnicka AR. Global variations and time trends in the prevalence of primary open angle glaucoma (POAG): a systematic review and meta-analysis. *Br J Ophthalmol*. 2016;100:86–93.
3. Gupta P, Zhao D, Guallar E, Ko F, Boland MV, Friedman DS. Prevalence of glaucoma in the United States: the 2005–2008 National Health and Nutrition Examination Survey. *Investig Ophthalmol Vis Sci*. 2016;57:2905–2913.
4. Heijl A, Leske MC, Bengtsson B, Hyman L, Bengtsson B, Hussein M. Reduction of intraocular pressure and glaucoma progression. *Arch Ophthalmol*. 2002;120:1268–1279.

5. Stamer WD, Acott TS. Current understanding of conventional outflow dysfunction in glaucoma. *Curr Opin Ophthalmol*. 2012;23:135–143.
6. Acott TS, Kelley MJ. Extracellular matrix in the trabecular meshwork. *Exp Eye Res*. 2008;86:543–561.
7. Acott TS, Kelley MJ, Keller KE, et al. Intraocular pressure homeostasis: maintaining balance in a high-pressure environment. *J Ocul Pharmacol Ther*. 2014;30:94–101.
8. Vranka JA, Kelley MJ, Acott TS, Keller KE. Extracellular matrix in the trabecular meshwork: Intraocular pressure regulation and dysregulation in glaucoma. *Exp Eye Res*. 2015;133:112–125.
9. Alvarado J, Murphy C, Juster R. Trabecular meshwork cellularity in primary open-angle glaucoma and nonglaucomatous normals. *Ophthalmology*. 1984;91:564–579.
10. Hoare MJ, Grierson I, Brotchie D, Pollock N, Cracknell K, Clark AF. Cross-linked actin networks (CLANs) in the trabecular meshwork of the normal and glaucomatous human eye in situ. *Investig Ophthalmol Vis Sci*. 2009;50:1255–1263.
11. Zode GS, Kuehn MH, Nishimura DY, et al. Reduction of ER stress via a chemical chaperone prevents disease phenotypes in a mouse model of primary open angle glaucoma. *J Clin Invest*. 2011;121:3542–3553.
12. Zhao J, Wang S, Zhong W, Yang B, Sun L, Zheng Y. Oxidative stress in the trabecular meshwork (review). *Int J Mol Med*. 2016;38:995–1002.
13. Rohen JW, Futa R, Liitjen-Drecoll E. The fine structure of the cribriform meshwork in normal and glaucomatous eyes as seen in tangential sections. *Investig Opthalmology Vis Sci*. 1981;21:574–585.
14. Vranka JA, Staverosky JA, Reddy AP, et al. Biomechanical rigidity and quantitative proteomics analysis of segmental regions of the trabecular meshwork at physiologic and elevated pressures. *Investig Ophthalmol Vis Sci*. 2018;59:246–259.
15. Last JA, Pan T, Ding Y, et al. Elastic modulus determination of normal and glaucomatous human trabecular meshwork. *Investig Ophthalmol Vis Sci*. 2011;52:2147–2152.
16. Raghunathan VK, Eaton JS, Christian BJ, et al. Biomechanical, ultrastructural, and electrophysiological characterization of the non-human primate experimental glaucoma model. *Sci Rep*. 2017;7:14329.
17. Lütjen-Drecoll E, Rittig M, Rauterberg J, Jander R, Mollenhauer J. Immunomicroscopical study of type VI collagen in the trabecular meshwork of normal and glaucomatous eyes. *Exp Eye Res*. 1989;48:139–147.
18. Medina-Ortiz WE, Belmares R, Neubauer S, Wordinger RJ, Clark AF. Cellular fibronectin expression in human trabecular meshwork and induction by transforming growth factor-β2. *Investig Ophthalmol Vis Sci*. 2013;54:6779–6788.
19. Wang K, Li G, Read AT, et al. The relationship between outflow resistance and trabecular meshwork stiffness in mice. *Sci Rep*. 2018;8:5848.
20. Raghunathan VK, Morgan JT, Park SA, et al. Dexamethasone stiffens trabecular meshwork, trabecular meshwork cells, and matrix. *Investig Ophthalmol Vis Sci*. 2015;56:4447–4459.
21. Tovar-Vidales T, Roque R, Clark AF, Wordinger RJ. Tissue transglutaminase expression and activity in normal and glaucomatous human trabecular meshwork cells and tissues. *Investig Ophthalmol Vis Sci*. 2008;49:622–628.
22. Sethi A, Mao W, Wordinger RJ, Clark AF. Transforming growth factor beta induces extracellular matrix protein cross-linking lysyl oxidase (LOX) genes in human trabecular meshwork cells. *Investig Ophthalmol Vis Sci*. 2011;52:5240–5250.
23. Raychaudhuri U, Millar JC, Clark AF. Tissue transglutaminase elevates intraocular pressure in mice. *Investig Ophthalmol Vis Sci*. 2017;58:6197–6211.
24. Raychaudhuri U, Millar JC, Clark AF, Clark AF. Knockout of tissue transglutaminase ameliorates TGFβ2-induced ocular hypertension: a novel therapeutic target for glaucoma? *Exp Eye Res*. 2018;171:106–110.
25. Yang YF, Sun YY, Acott TS, Keller KE. Effects of induction and inhibition of matrix cross-linking on remodeling of the aqueous outflow resistance by ocular trabecular meshwork cells. *Sci Rep*. 2016;6:30505.
26. Thorleifsson G, Magnusson KP, Sulem P, et al. Common sequence variants in the LOXL1 gene confer susceptibility to exfoliation glaucoma. *Science* 2007;317:1397–1400.
27. Maki J. Lysyl oxidases in mammalian development and certain pathological conditions. *Histol Histopathol*. 2009;24:651–660.
28. Lorand L, Graham RM, Street V. Transglutaminases: crosslinking enzymes with pleiotropic functions. *Nat Rev Mol Cell Biol*. 2003;4:140–156.
29. Rodriguez C, Rodriguez-Sinovas A, J M-G. Lysyl oxidase as a potential therapeutic target. *Drug News Perspect*. 2008;21:218–224.
30. Kasetti RB, Maddineni P, Millar JC, Clark AF, Zode GS. Increased synthesis and deposition of extracellular matrix proteins leads to endoplasmic reticulum stress in the trabecular meshwork. *Sci Rep*. 2017;7:14951.
31. Steppan J, Sikka G, Jandu S, et al. Exercise, vascular stiffness, and tissue transglutaminase. *J Am Hear Assoc*. 2014;3:1–10.
32. Steppan J, Bergman Y, Viegas K, et al. Tissue transglutaminase modulates vascular stiffness and function through crosslinking-dependent and crosslinking-independent functions. *J Am Hear Assoc*. 2017;6:1–15.
33. Kim GI, Gil C, Seo J, et al. Mechanotransduction of human pluripotent stem cells cultivated on tunable cell-derived extracellular matrix. *Biomaterials*. 2018;150:100–111.
34. Dupont S, Morsut L, Aragona M, et al. Role of YAP/TAZ in mechanotransduction. *Nature*. 2011;474:179–184.
35. Du J, Zu Y, Li J, et al. Extracellular matrix stiffness dictates Wnt expression through integrin pathway. *Sci Rep*. 2016;6:20395.
36. Pocaterra A, Romani P, Dupont S. YAP/TAZ functions and their regulation at a glance. *J Cell Sci*. 2020;133:jcs230425.
37. Barbolina MV, Liu Y, Gurler H, et al. Matrix rigidity activates Wnt signaling through down-regulation of dickkopf-1 protein. *J Biol Chem*. 2013;288:141–151.
38. Imajo M, Miyatake K, Iimura A, Miyamoto A, Nishida E. A molecular mechanism that links Hippo signalling to the inhibition of Wnt/β-catenin signalling. *EMBO J*. 2012;31:1109–1122.
39. Varelas X, Miller BW, Sopko R, et al. The Hippo pathway regulates Wnt/β-catenin signaling. *Dev Cell*. 2010;18:579–591.
40. Azzolin L, Panciera T, Soligo S, et al. YAP/TAZ incorporation in the β-catenin destruction complex orchestrates the Wnt response. *Cell*. 2014;158:157–170.
41. Azzolin L, Zanconato F, Bresolin S, et al. Role of TAZ as mediator of Wnt signaling. *Cell*. 2012;151:1443–1456.
42. Park HW, Kim YC, Yu B, et al. Alternative Wnt signaling activates YAP/TAZ. *Cell*. 2015;162:780–794.
43. Heallen T, Zhang M, Wang J, et al. Hippo pathway inhibits Wnt signaling to restrain cardiomyocyte proliferation and heart size. *Science*. 2011;332:458–461.
44. Cai J, Maitra A, Anders RA, Taketo MM, Pan D. β-catenin destruction complex-independent regulation of Hippo-YAP signaling by APC in intestinal tumorigenesis. *Genes Dev*. 2015;29:1493–1506.
45. Sasaki H. Roles and regulations of Hippo signaling during preimplantation mouse development. *Dev Growth Differ*. 2017;59:12–20.

Investigative Ophthalmology & Visual Science

46. Hossain Z, Ali SM, Hui LK, et al. Glomerulocystic kidney disease in mice with a targeted inactivation of Wwtr1. *Proc Natl Acad Sci USA*. 2007;104:1631–1636.
47. Raghunathan VK, Morgan JT, Dreier B, et al. Role of substratum stiffness in modulating genes associated with extracellular matrix and mechanotransducers YAP and TAZ. *Investig Ophthalmol Vis Sci*. 2013;54:378–386.
48. Mao W, Cameron Millar J, Wang WH, et al. Existence of the canonical Wnt signaling pathway in the human trabecular meshwork. *Investig Ophthalmol Vis Sci*. 2012;53:7043–7051.
49. Wang WH, McNatt LG, Pang IH, et al. Increased expression of the WNT antagonist sFRP-1 in glaucoma elevates intraocular pressure. *J Clin Invest*. 2008;118:1056–1064.
50. Morgan JT, Raghunathan VK, Chang YR, Murphy CJ, Russell P. Wnt inhibition induces persistent increases in intrinsic stiffness of human trabecular meshwork cells. *Exp Eye Res*. 2015;132:174–178.
51. Webber HC, Bermudez JY, Millar JC, Mao W, Clark AF. The role of Wnt / β-catenin signaling and K-cadherin in the regulation of intraocular pressure. *Invest Ophthalmol Vis Sci*. 2018;59:1454–1466.
52. Ho LTY, Skiba N, Ullmer C, Rao PV. Lysophosphatidic acid induces ECM production via activation of the mechanosensitive Yap/Taz transcriptional pathway in trabecular meshwork cells. *Investig Ophthalmol Vis Sci*. 2018;59:1969–1984.
53. Sung HW, Huang RN, Huang LH, Tsai CC. In vitro evaluation of cytotoxicity of a naturally occurring cross-linking reagent for biological tissue fixation. *J Biomater Sci Polym Ed*. 1999;10:63–78.
54. Tsai C, Huang R, Sung H, Liang HC. In vitro evaluation of the genotoxicity of a naturally occurring crosslinking agent (genipin) for biologic tissue fixation. *J Biomed Mater Res*. 2000;52:58–65.
55. Sung H, Huang R, Huang LLH, Tsai C, Chiu C. Feasibility study of a natural crosslinking reagent for biological tissue fixation. *J Biomed Mater Res*. 1998;42:560–567.
56. Yemanyi F, Vranka JA, Raghunathan V. Crosslinked ECM modulates β-Catenin and YAP/TAZ pathways in human trabecular meshwork cells. *Invest Ophthalmol Vis Sci*. 2020;61:1434.
57. Keller KE, Bhattacharya SK, Borrás T, et al. Consensus recommendations for trabecular meshwork cell isolation, characterization and culture. *Exp Eye Res*. 2018;171:164–173.
58. Stamer WD, Clark AF. The many faces of the trabecular meshwork cell. *Exp Eye Res*. 2017;158:112–123.
59. Yemanyi F, Vranka J, Raghunathan VK. Generating cell-derived matrices from human trabecular meshwork cell cultures for mechanistic studies. *Methods Cell Biol*. 2020;156:271–307.
60. Kaukonen R, Jacquemet G, Hamidi H, Ivaska J. Cell-derived matrices for studying cell proliferation and directional migration in a complex 3D microenvironment. *Nat Protoc*. 2017;12:2376–2390.
61. Raghunathan VK, Benoit J, Kasetti R, et al. Glaucomatous cell derived matrices differentially modulate non-glaucomatous trabecular meshwork cellular behavior. *Acta Biomater*. 2018;71:444–459.
62. Raghunathan VK, Morgan JT, Chang Y, et al. Transforming growth factor beta 3 modifies mechanics and composition of extracellular matrix deposited by human trabecular meshwork cells. *ACS Biomater Sci Eng*. 2015;1:110–118.
63. Chang YR, Raghunathan VK, Garland SP, Morgan JT, Russell P, Murphy CJ. Automated AFM force curve analysis for determining elastic modulus of biomaterials and biological samples. *J Mech Behav Biomed Mater*. 2014;37:209–218.
64. Výborný K, Vallová J, Kočí Z, et al. Genipin and EDC crosslinking of extracellular matrix hydrogel derived from human umbilical cord for neural tissue repair. *Sci Rep*. 2019;9:10674.
65. Gao M, Wang Y, He Y, et al. Comparative evaluation of decellularized porcine liver matrices crosslinked with different chemical and natural crosslinking agents. *Xenotransplantation*. 2019;26:e12470.
66. Engler AJ, Sen S, Sweeney HL, Discher DE. Matrix Elasticity directs stem cell lineage specification. *Cell*. 2006;126:677–689.
67. Schlunck G, Han H, Wecker T, Kampik D, Meyer-ter-Vehn T, Grehn F. Substrate rigidity modulates cell-matrix interactions and protein expression in human trabecular meshwork cells. *Investig Ophthalmol Vis Sci*. 2008;49:262–269.
68. Bordeleau F, Lapierre ME, Sheng Y, Marceau N. Keratin 8/18 regulation of cell stiffness-extracellular matrix interplay through modulation of rho-mediated actin cytoskeleton dynamics. *PLoS One*. 2012;7:e38780.
69. Webber HC, Bermudez JY, Sethi A, Clark AF, Mao W. Crosstalk between TGFβ and Wnt signaling pathways in the human trabecular meshwork. *Exp Eye Res*. 2016;148:97–102.
70. Villarreal G, Chatterjee A, Oh SS, Oh DJ, Kang MH, Rhee DJ. Canonical Wnt signaling regulates extracellular matrix expression in the trabecular meshwork. *Investig Ophthalmol Vis Sci*. 2014;55:7433–7440.
71. Nusse R, Clevers H. Wnt/β-catenin signaling, disease, and emerging therapeutic modalities. *Cell*. 2017;169:985–999.
72. Makita R, Uchijima Y, Nishiyama K, et al. Multiple renal cysts, urinary concentration defects, and pulmonary emphysematous changes in mice lacking TAZ. *Am J Physiol - Ren Physiol*. 2008;294:F542–F553.
73. Byfield FJ, Reen RK, Shentu T, Levitan I, Gooch KJ. Endothelial actin and cell stiffness is modulated by substrate stiffness in 2D and 3D. *J Biomech*. 2009;42:1114–1119.
74. Rice AJ, Cortes E, Lachowski D, et al. Matrix stiffness induces epithelial-mesenchymal transition and promotes chemoresistance in pancreatic cancer cells. *Oncogenesis*. 2017;6:e352.
75. Discher DE, Janmey P, Wang YL. Tissue cells feel and respond to the stiffness of their substrate. *Science*. 2005;310:1139–1143.
76. Overby DR, Zhou EH, Vargas-Pinto R, et al. Altered mechanobiology of Schlemm's canal endothelial cells in glaucoma. *Proc Natl Acad Sci USA*. 2014;111:13876–13881.
77. Clevers H. Wnt/β-catenin signaling in development and disease. *Cell*. 2006;127:469–480.
78. Tripathi RC, Li J, Chan WFA, Tripathi BJ. Aqueous humor in glaucomatous eyes contains an increased level of TGF-β2. *Exp Eye Res*. 1994;59:723–728.
79. Inatani M, Tanihara H, Katsuta H, Honjo M, Kido N, Honda Y. Transforming growth factor- β2 levels in aqueous humor of glaucomatous eyes. *Graefe's Arch Clin Exp Ophthalmol*. 2001;239:109–113.
80. Dhamodaran K, Baidouri H, Sandoval L, Raghunathan V. Wnt activation after inhibition restores trabecular meshwork cells toward a normal phenotype. *Investig Opthalmology Vis Sci*. 2020;61:30.
81. Matsunaga M, Hatta K, Nagafuchi A, Takeichi M. Guidance of optic nerve fibres by N-cadherin adhesion molecules. *Nature*. 1988;334:62–64.
82. Auersperg N, Pan J, Grove BD, et al. E-cadherin induces mesenchymal-to-epithelial transition in human ovarian surface epithelium. *Proc Natl Acad Sci USA*. 1999;96:6249–6254.
83. Tzima E, Irani-Tehrani M, Kiosses WB, et al. A mechanosensory complex that mediates the endothelial cell response to fluid shear stress. *Nature*. 2005;437:426–431.

Investigative Ophthalmology & Visual Science

84. Kotini M, Barriga EH, Leslie J, et al. Gap junction protein Connexin-43 is a direct transcriptional regulator of N-cadherin in vivo. *Nat Commun*. 2018;9:3846.
85. Nagy JI, Lynn BD. Structural and intermolecular associations between connexin36 and protein components of the adherens junction–neuronal gap junction complex. *Neuroscience*. 2018;384:241–261.
86. Muppala S, Raghunathan VK, Jalilian I, Thomasy S, Murphy CJ. YAP and TAZ are distinct effectors of corneal myofibroblast transformation. *Exp Eye Res*. 2019;180:102–109.
87. Tang C, Takahashi-Kanemitsu A, Kikuchi I, Ben C, Hatakeyama M. Transcriptional co-activator functions of YAP and TAZ are inversely regulated by tyrosine phosphorylation status of parafibromin. *iScience*. 2018;1:1–15.
88. Moreno-Vicente R, Pavón DM, Martín-Padura I, et al. Caveolin-1 modulates mechanotransduction responses to substrate stiffness through actin-dependent control of YAP. *Cell Rep*. 2018;25:1622–1635.
89. Rausch V, Bostrom JR, Park J, et al. The Hippo pathway regulates caveolae expression and mediates flow response via caveolae. *Curr Biol*. 2019;29:242–255.
90. Rubin J, Schwartz Z, Boyan BD, et al. Caveolin-1 knockout mice have increased bone size and stiffness. *J Bone Miner Res*. 2007;22:1408–1418.
91. Elliott MH, Ashpole NE, Gu X, et al. Caveolin-1 modulates intraocular pressure: implications for caveolae mechanoprotection in glaucoma. *Sci Rep*. 2016;6:37127.

Amended August 25, 2020: In the Figure 11 legend, the words "(Right cellular compartment)" and "(Left cellular compartment)" have been switched to move them to the correct locations in the legend.